REPORT NO. FAA-RD-81-43

ASDE-3 ANTENNA DEVELOPMENT AND TEST

Francis J. LaRussa

U.S. DEPARTMENT OF TRANSPORTATION
Research and Special Programs Administration
Transportation Systems Center
Cambridge MA 02142

JANUARY 1981
FINAL REPORT

Prepared by

U.S. DEPARTMENT OF TRANSPORTATION
FEDERAL AVIATION ADMINISTRATION
Systems Research and Development Service
Washington DC 20590

Technical Report Documentation Page

1. Report No.	2. Government Accession No.	3. Recipient's Catalog No.
FAA-RD-81-43		

4. Title and Subtitle	5. Report Date
ASDE-3 ANTENNA DEVELOPMENT AND TEST	April 1981
	6. Performing Organization Code: DOT/TSC/541
7. Author(s): Francis J. LaRussa	8. Performing Organization Report No.: DOT-TSC-FAA-81-10
9. Performing Organization Name and Address: U.S.Department of Transportation, Transportation Systems Center, Cambridge MA 02142	10. Work Unit No. (TRAIS): FA121/R1135
	11. Contract or Grant No.
12. Sponsoring Agency Name and Address: U.S.Department of Transportation, Federal Aviation Administration, Systems Research and Development Service, Washington DC 20590	13. Type of Report and Period Covered: Jan 1980-April 1981
	14. Sponsoring Agency Code

15. Supplementary Notes

16. Abstract

The ASDE-3 radar antenna was developed so that closely spaced targets on an airport surface could be resolved. The requirement of accurately detecting targets as close as 500 feet from the antenna necessitated some type of near field focussing. A variable focus, shaped beam, doubly curved reflector was designed and successfully tested for this application. Additional features included an integrated rotating radome and circular polarization. Representative azimuth and elevation patterns are presented. During the development, a method for taking and plotting radiation patterns of the antenna scanning at its operational rotation rate was devised and is described.

17. Key Words	18. Distribution Statement
ASDE, Airport Surface Detection	DOCUMENT IS AVAILABLE TO THE PUBLIC THROUGH THE NATIONAL TECHNICAL INFORMATION SERVICE, SPRINGFIELD, VIRGINIA 22161

19. Security Classif. (of this report)	20. Security Classif. (of this page)	21. No. of Pages	22. Price
Unclassified	Unclassified	74	

Form DOT F 1700.7 (8-72) Reproduction of completed page authorized

TABLE OF CONTENTS

LIST OF ILLUSTRATION

LIST OF ILLUSTRATIONS (CONT.)

LIST OF ILLUSTRATIONS (CONT.)

LIST OF TABLES

1. INTRODUCTION

One of the major components of the ASDE-3 Radar development was the variable focus antenna with integral rotating radome, or rotodome. The integral configuration was developed to address the problems of a large overturning moment and possible radiation pattern perturbation, associated with large fixed spherical radomes. This report details the development of the antenna and is part of the technical data package written to support the following stage 4 spectrum approval item.

Representative data and antenna radiation patterns in both azimuth and elevation planes are presented.

2. GENERAL DISCUSSION

2.1 REQUIREMENTS

The ASDE-3 antenna azimuth beamwidth requirement of 0.25° with sidelobes greater than 20 dB below the peak of the beam, required an aperture of 280 wavelengths. At 16 GHz, the near field of such an antenna extended out to 4800 feet. To detect targets as close in as 500 feet, azimuthal focussing was necessary in order to avoid the deterioration of gain and beamwidth associated with near field effects.

Once the horizontal aperture was established, the choice of vertical aperture was dictated by the required peak gain and vertical directivity set by the system rainfall performance requirements. A vertical aperture of about 80 wavelengths was chosen to provide a vertical beamwidth of 1.6° with elevation beam shaping. The choice of beam shape involved a tradeoff between peak gain at elevation boresight (affecting target returns at maximum range) and gain at large depression angles (corresponding to targets at close range). Figure 1 shows the peak gain and close-in gain reduction for some of the more simple beam shapes. The angular extent of the shaping was dictated by the requirement to detect targets as close-in as 500 feet from the ASDE-3 towers whose heights vary and which can be as high as 300 feet above the airport surface. This latter worst case condition set the lower limit of the shaped beam at -31°. The theoretical elevation beam shape finally chosen is shown as the ASDE-3 curve in Figure 1 and has the following contour.

Elevation Angle	Beam Shape
+ 0.8° to - 0.8°	pencil beam
-0.8° to -3.2°	$\csc^{1.5}$
-3.2° to -31°	csc

The requirement for circular polarization was established by the need to reduce rain clutter return.

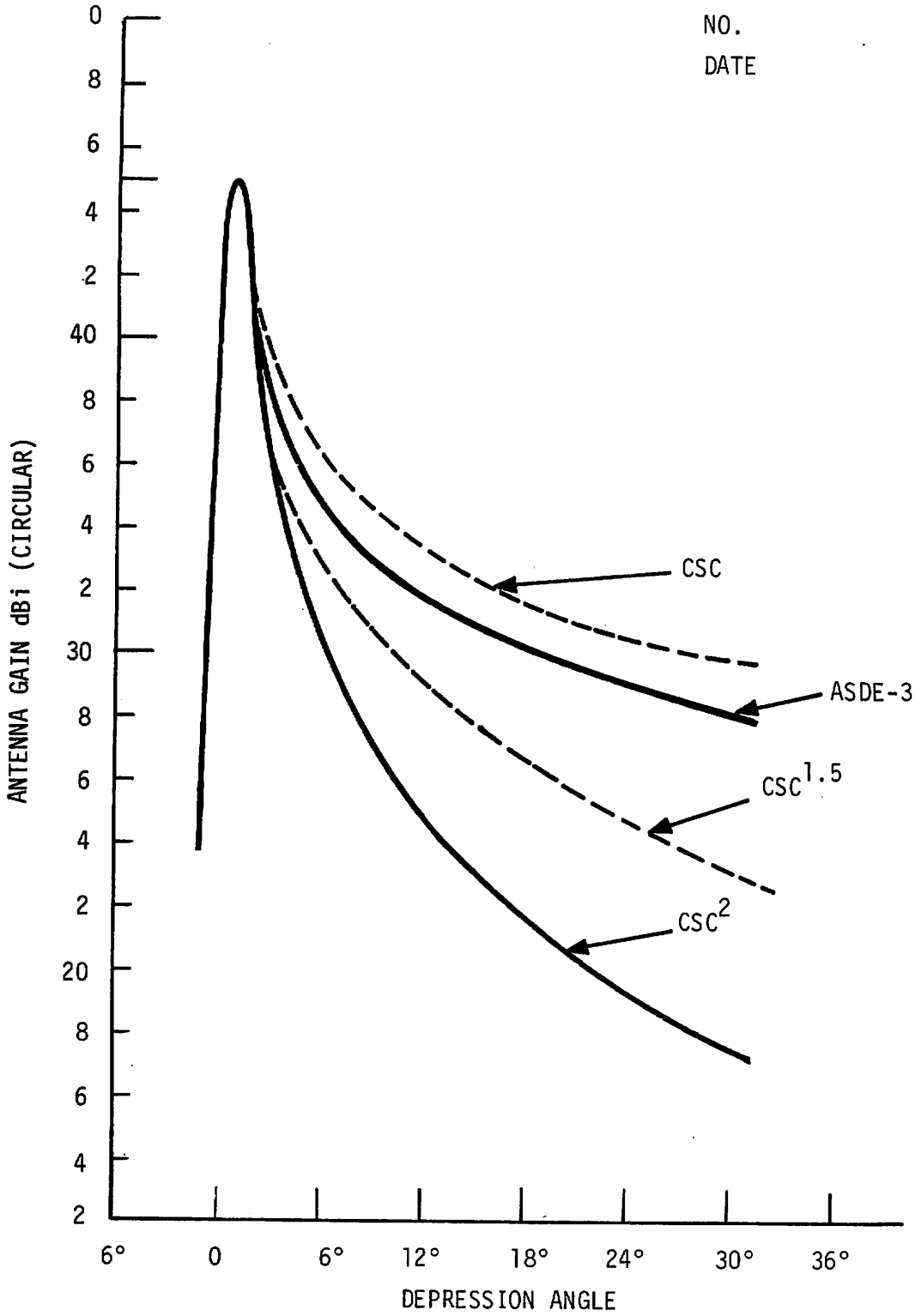

FIGURE 1. POSSIBLE ELEVATION BEAM SHAPES FOR AIRPORT SURFACE SURVEILLANCE

2.2 DESIGN APPROACH

The near field problem and elevation beam requirement were uniquely solved with a single-feed, doubly-curved reflector design. The solution is a shaped-beam, variable-focus reflector antenna which has a series of elliptical contours whose eccentricities vary with depression angle. In this technique, the feed horn is located at the primary foci of these ellipses. The major axes are slant ranges from the tower and the conjugate foci lie on the airport surface at different ranges. Figure 2 illustrates this technique. This is a departure from the conventional technique of focussing a parabolic reflector to some point in the near field and accepting whatever deterioration that occurs outside this region.

The antenna is enclosed in a spheroidal radome that rotates with the antenna and is aerodynamically shaped to minimize drag. This approach accomplished two objectives. It reduced the overturning moment of the roof equipment and the rotating radome (rotodome) shed rain and helped reduce the deleterious effects that a thin film of water has on the microwave radiation at these frequencies.

Both the antenna and radome are fabricated of fiberglass and resin. The reflector is a composite sandwich consisting of a flexible aluminum honeycomb core sandwiched between layers of resin impregnated fiberglass, and aluminum screening. The screening was to be the reflecting surface, but variations in resin thickness could introduce slight phase variations in the reflected microwave energy with consequent gain and side lobe deterioration. Therefore, the decision was made to paint the reflecting surface with silver paint. Figure 3 shows a cross-section of the reflector. The sandwich is layered symmetrically about the flexible core to preclude distortions during fabrication and resin cure.

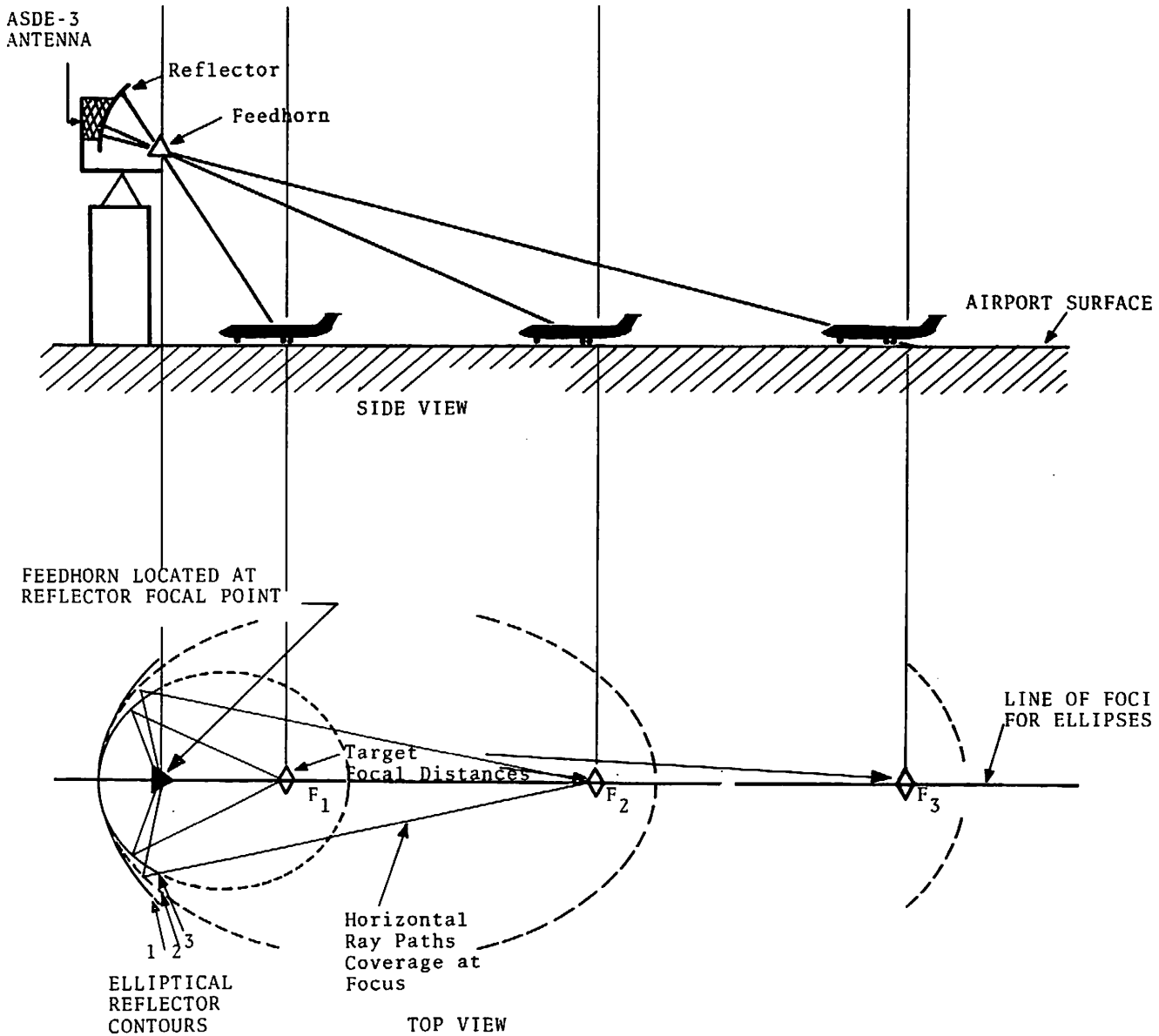

FIGUPE 2. VARIABLE AZIMUTHAL FOCUSSING USING CONFOCAL ELLIPSES

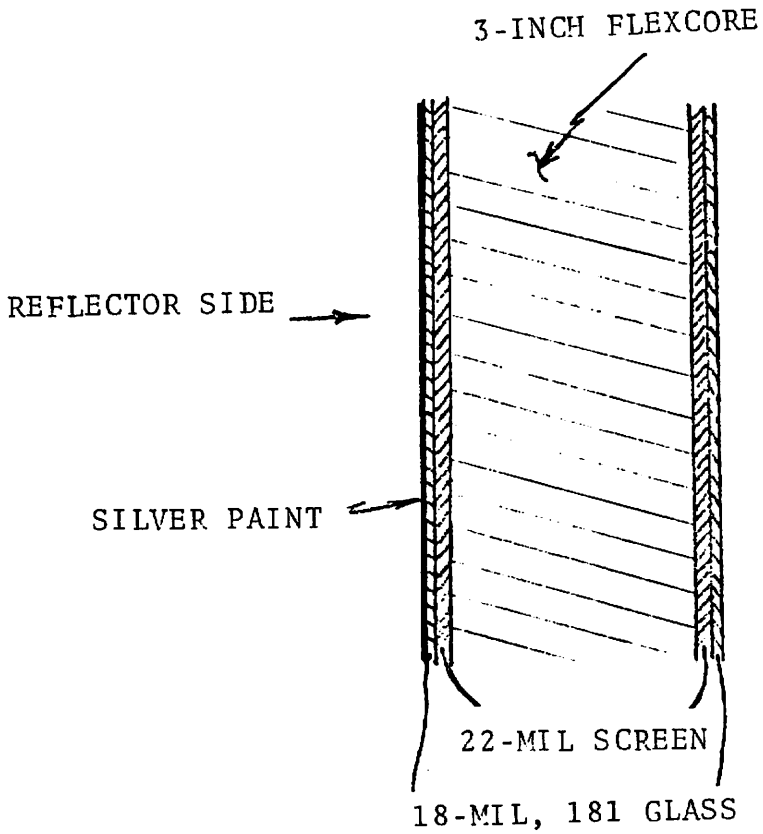

FIGURE 3. ANTENNA SANDWICH CONSTRUCTION

The radome is also fabricated of fiberglass and resin. The roof and floor sections are cored fiberglass sandwich sections which are bolted together. The wall which is the window for the microwave energy is a solid fiberglass laminate approximately one half wavelength thick in the material and which is optimized for an incidence angle of about 60°. The radome window area is coated with Gelcoat to prevent the surface from building up a film of water during rainstorms.

3. VERIFICATION OF DESIGN

3.1 PRELIMINARY TESTS

Prior to building the full-scale antenna, a small 1/3-scale antenna having the same aspect ratio but having a different shaped beam sector was built and tested by Microwave Specialty Corp. (MSC). Changing the extent of the shaped beam sector was necessary because scaling the 31° sector would have resulted in an elevation beam in excess of 90° which is virtually imposible to design or build. The variable focus feature was qualitatively verified but because of the difficulties in scaling, the model yielded very little quantitative data.

The first antenna built and tested by MSC was of poor quality. Problems and errors during the fabrication process resulted in an antenna that had very poor azimuth side lobes. The antenna did appear to exhibit the effects of focussing since in the near field, the beamwidth in the vicinity of the beam peak (focussed for the far field) exhibited severe beam broadening and high side lobes. At large depression angles (focussed for the near-field), the near-field azimuth patterns appeared to improve. Beamwidths narrowed to their approximate design values but the high side lobes persisted.

Far-field azimuth patterns in the vicinity of the beam peak showed similar narrow beamwidths close to the design values but with high side lobes. Far-field patterns at large depression angles could not be taken so that the defocussing could not be compared with the near-field case.

Despite the poor radiation patterns, the rotodome was accepted and delivered to the Cardion plant, where it was accidentally destroyed by fire.

Prior to the fire, when the range test results indicated poor antenna performance, separate studies were initiated by Teledyne Micronetics and by TSC to determine the cause of the

high side lobe levels and also to verify the design. The TSC study was contracted out to Texas Instruments (T.I.) of Dallas, Texas who had on hand a computer program, that could plot antenna radiation patterns using the actual fabrication dimensions of the reflector contour and the primary pattern of the feed horn. The Teledyne Micronetics study was independent of the TSC study but its objectives and approach were similar to the T.I. study. Both analyses arrived at the same conclusion, namely, that the antenna design had no fundamental flaws and that if built to the design dimensions should produce azimuth beamwidths on the order of 0.25° with side-lobe levels greater than 20 dB below peak of the beam at the focussed ranges. A more detailed analysis of the results of both studies is given in Section 3.2.

3.2 COMPUTER ANALYSES

The analyses performed by Texas Instruments (T.I.) and Teledyne Micronetics (T.M.) were both concerned with verifying the antenna design and assuring that the reflector contour was indeed correct for producing the specified radiation characteristics. The starting points for both studies were the primary patterns of the actual feed horn used for the antenna and the coordinates of the reflector surface. These data were used to generate aperture distributions from which radiation patterns were computed.

The T.I. analysis was programmed for generating only the far-field radiation patterns, so that the near-field variable focussing could not be verified. However, defocussing at large depression angles was observed in the calculated far-field azimuth and elevation patterns. The azimuthal beamwidths increased from 0.21° at beam peak to 0.61° at a depression angle of 25°. In addition, the computed gain dropped off more rapidly than the designed "shaped beam roll off" at the larger depression angles. Figure 4 shows the T.I. computed far-field broadening and decreased gain of the calculated azimuth beams. Figure 5 shows the specified elevation beam shape with the defocussed far-field

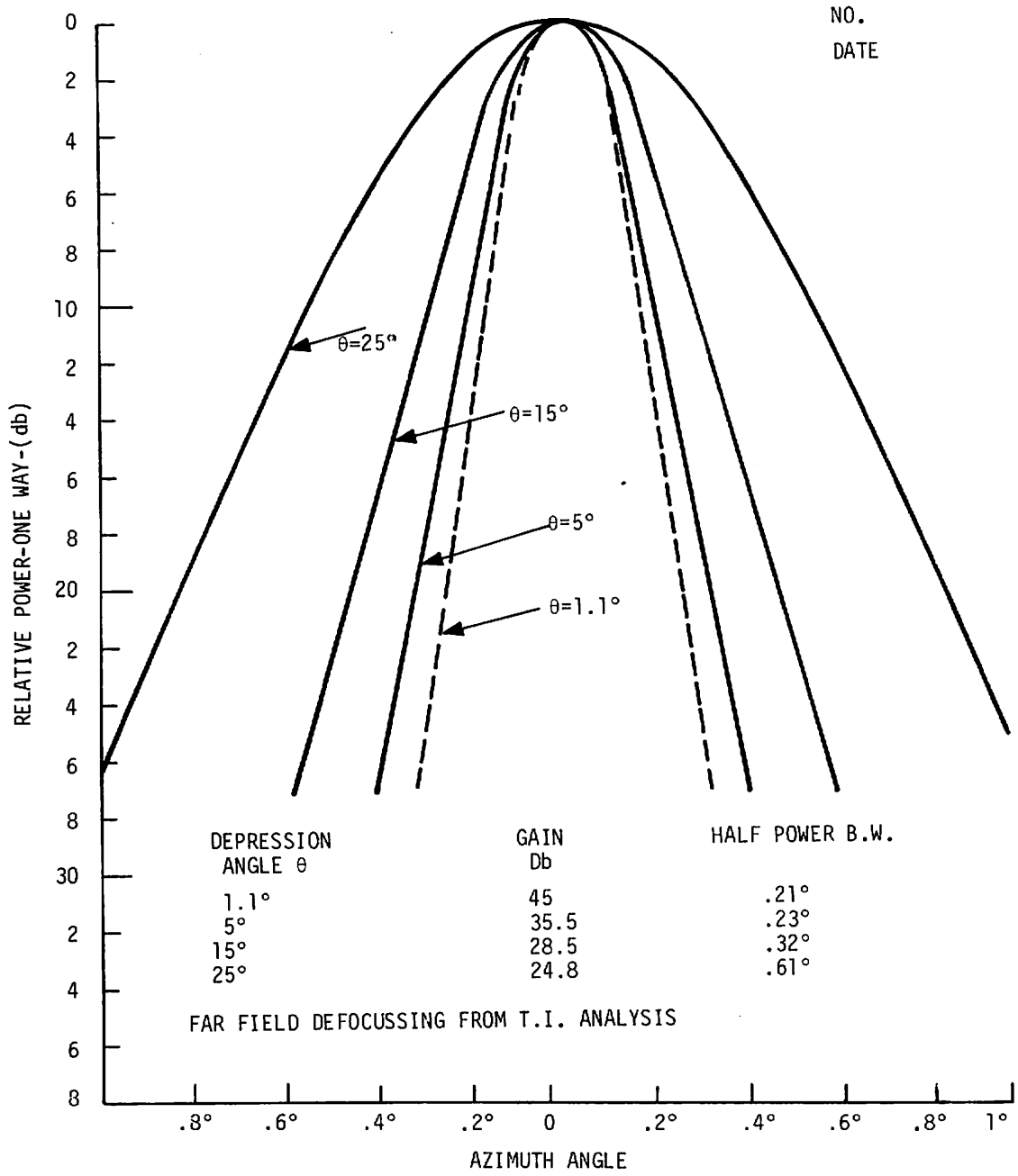

FIGURE 4. CALCULATED AZIMUTH FAR FIELD BEAMWIDTH VARIATION WITH DEPRESSION ANGLE

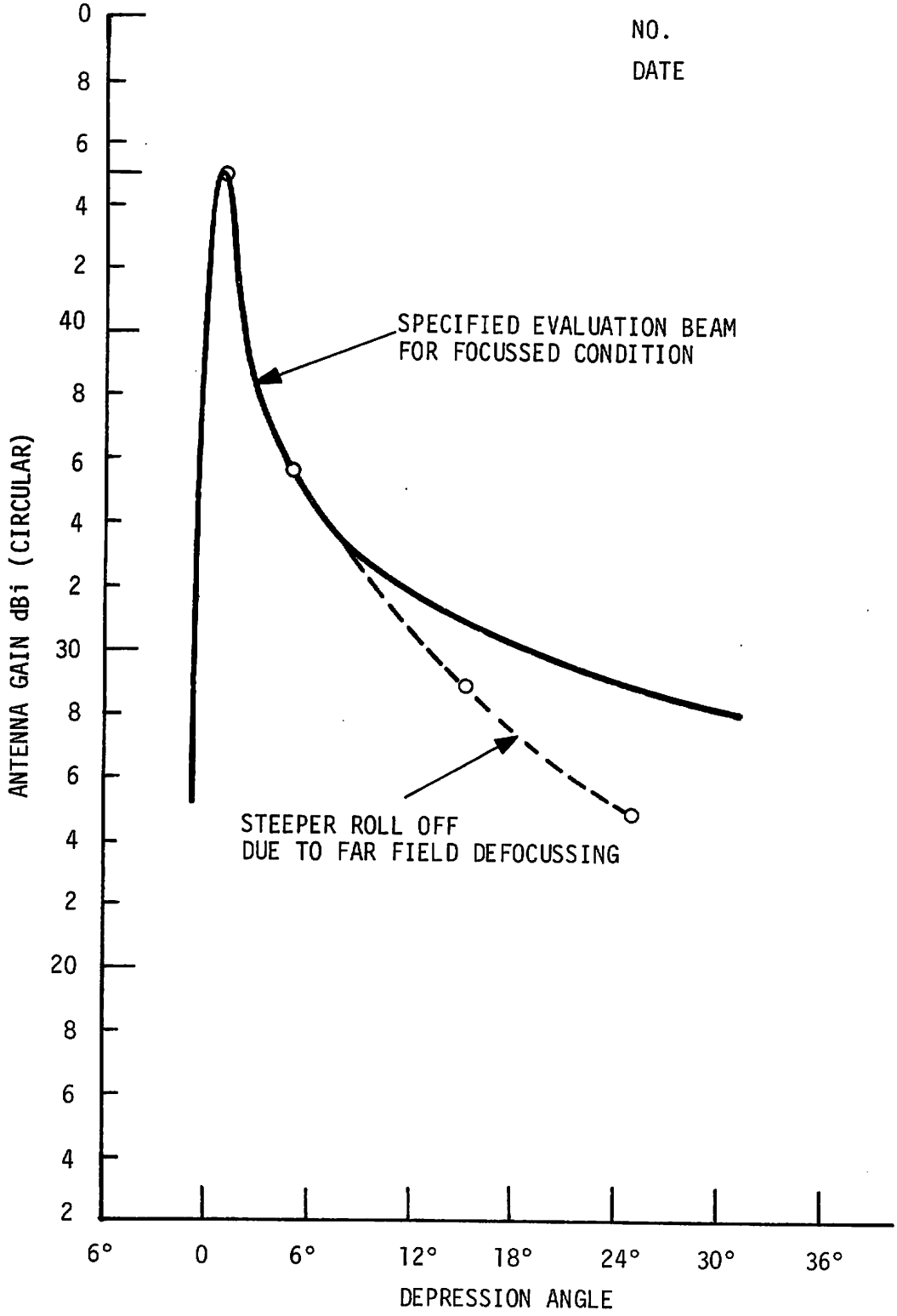

FIGURE 5. CALCULATED FAR FIELD GAIN AT VARIOUS DEPRESSION ANGLES

gain points. Similar results were observed in the TM analysis. In addition their analysis included a near field azimuth pattern computed for the peak of the elevation beam. Figure 6 shows the severe defocussing effects that occur in the near-field, as computed by T.M.

Both analyses used the primary feed horn patterns which are shown in Figures 7 and 8 in their computations. In a more detailed analysis T.I. concluded that the poor axial ratios of the feed horn patterns were due to a lack of coincidence of the phase centers of the two linearly polarized orthogonal components. This condition results in a cumulative phase error across the aperture and consequent poor axial ratios in the far field radiation patterns. In addition, as a consequence of calculating the radiation patterns, they found that the feed horn did not produce equal amplitude orthogonal components but rather the horizontal component was about 1.3 dB below the vertical component, and that the two components were not orthogonal. These factors tended to degrade the axial ratio, and hence the feed horn design is an area for improvement.

Despite a less than optimum feed horn, the analyses verified the ASDE-3 reflector design. The computed beamwidth and side-lobe levels indicated that with proper fabrication, the antenna would meet specification. The variable azimuth focus feature combined with a shaped elevation beam, using only a single feed appeared feasible. Limitations of the existing computer programs and the lack of time and funds did not permit a thorough investigation of this feature. However, the limited data from both the T.I. and T.M. analyses clearly showed defocussing effects with depression angle. T.I.'s limited analysis of phase front curvature, Figure 9 shows a variation with depression angle. This coupled with the defocussing effects observed in the"near-field-far field" gain and beamwidth comparisons appeared to imply feasibility and proper design for this feature. The poor performance of the first reflector was, therefore, ascribed to poor fabrication techniques which resulted in excessive tolerance build-up.

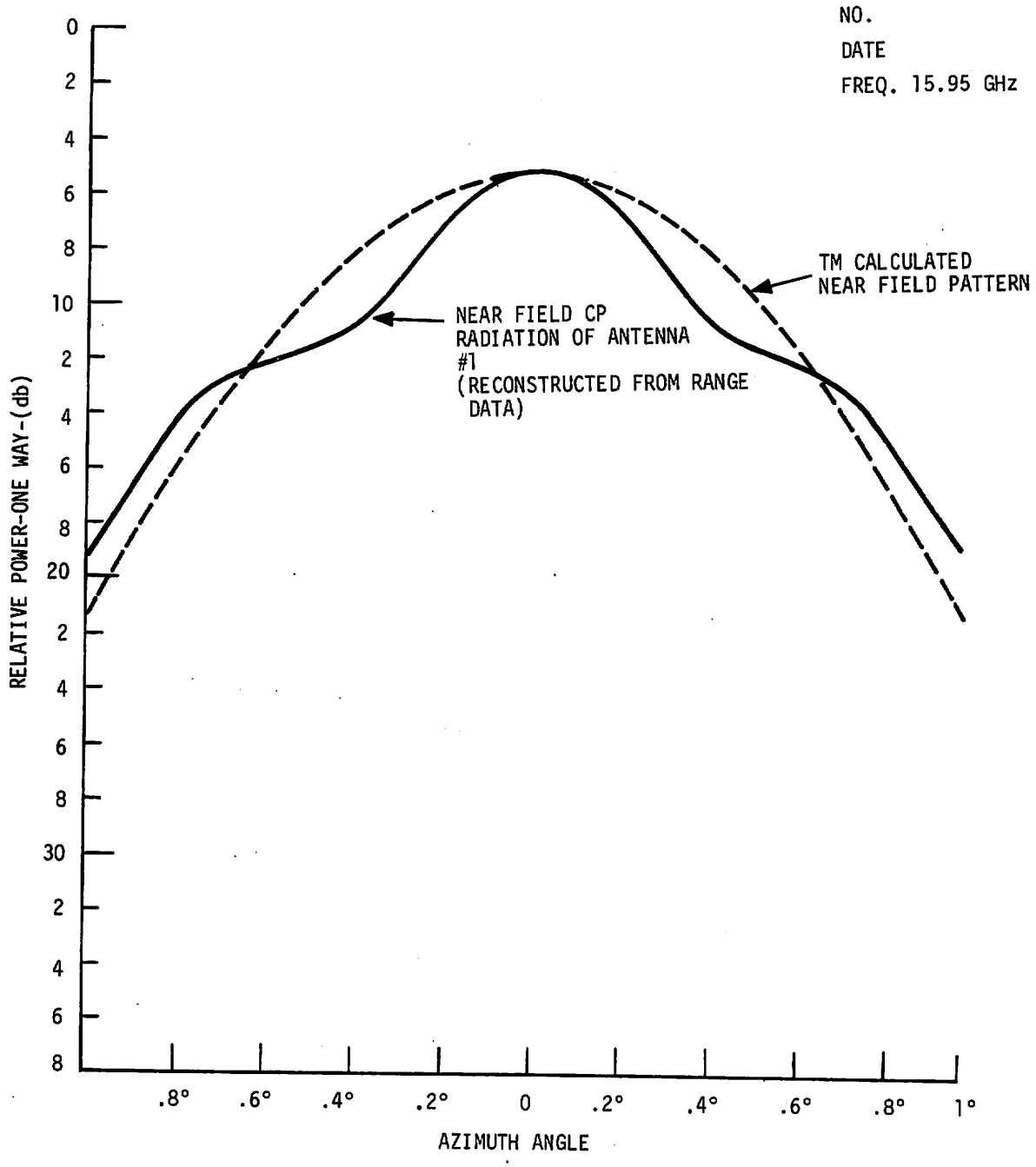

FIGURE 6. NEAR FIELD AZIMUTH DEFOCUSSING AT PEAK OF ELEVATION BEAM

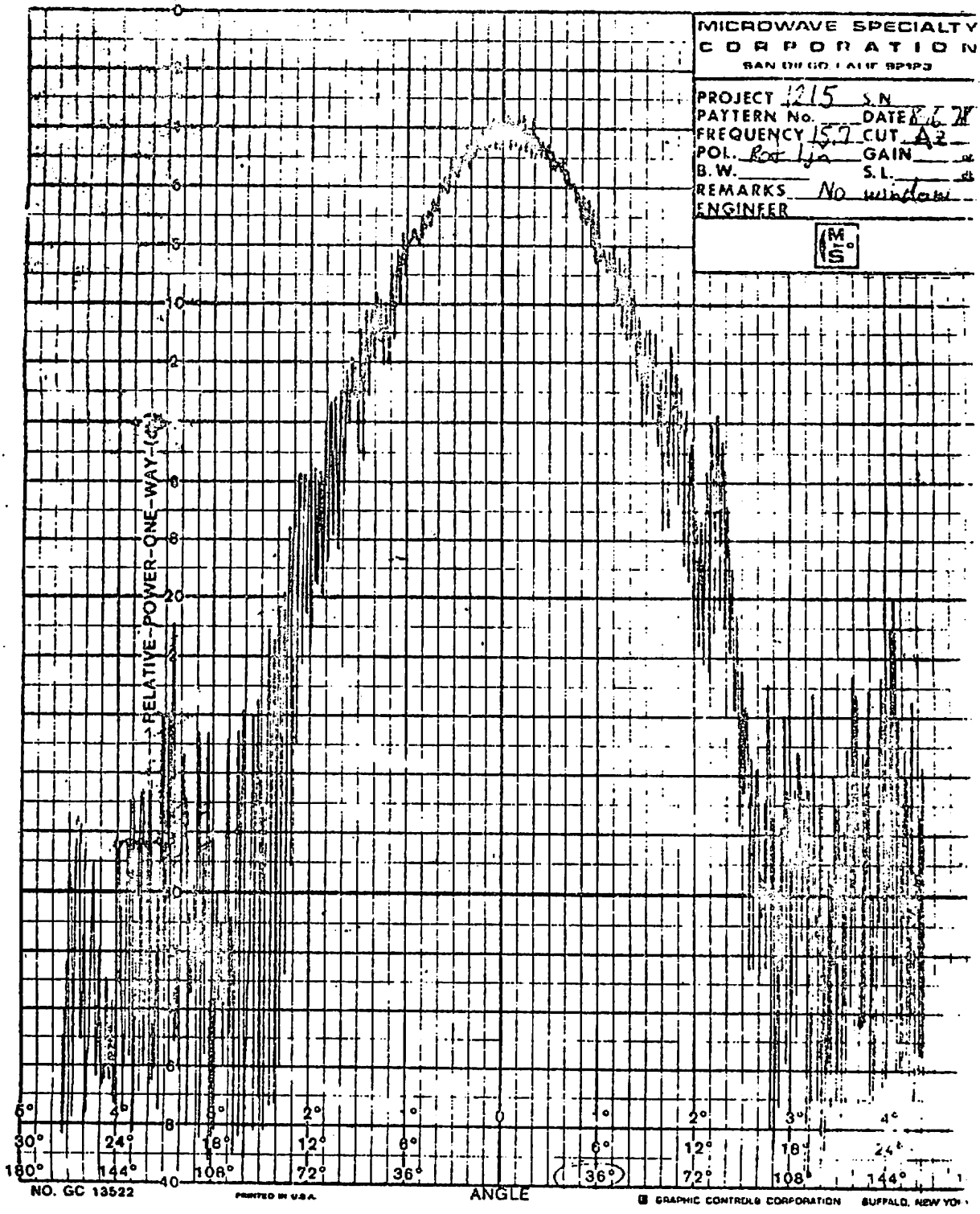

FIGURE 7. AZIMUTH PATTERN OF ASDE-3 ANTENNA FEED HORN

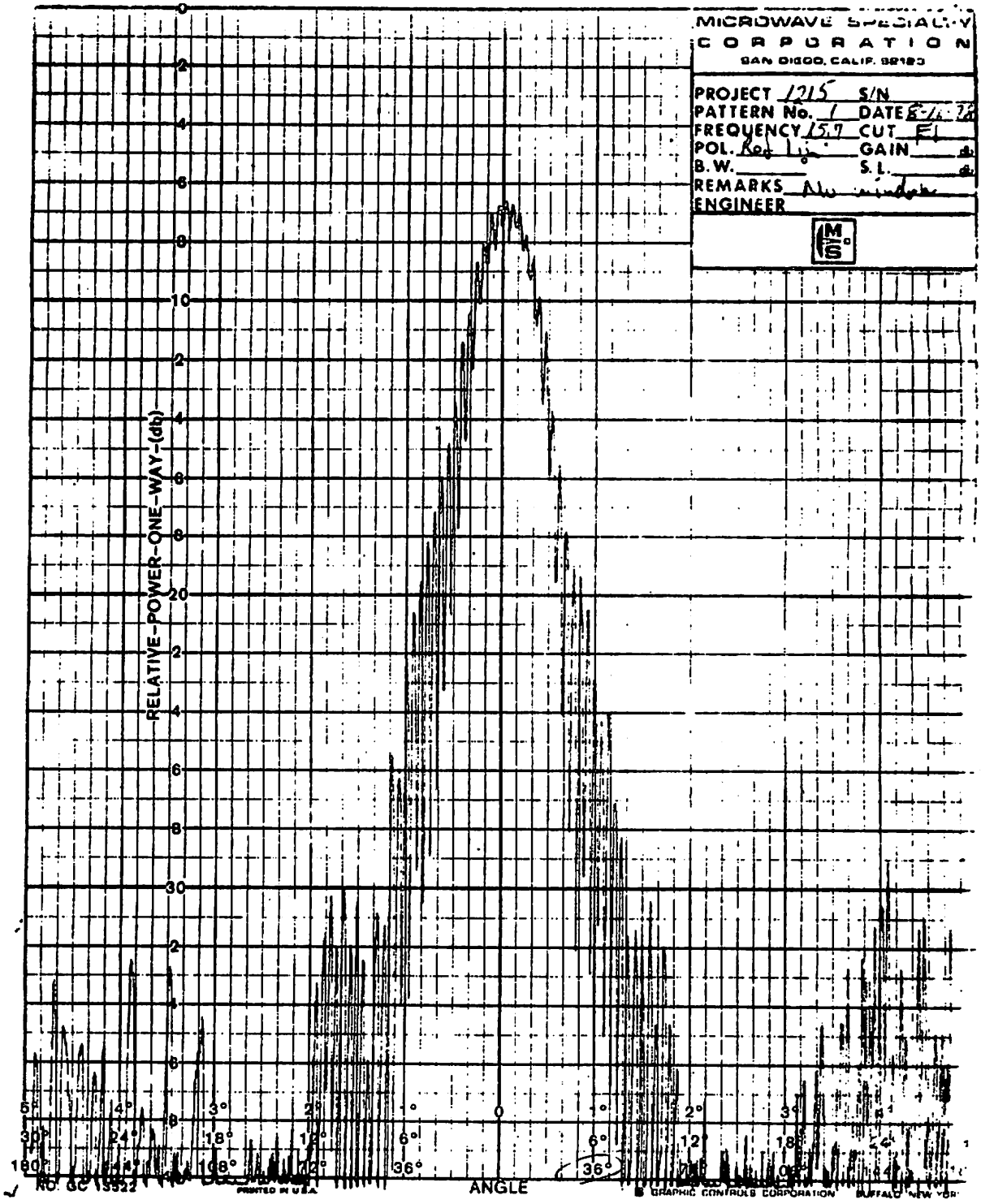

FIGURE 8. ELEVATION PATTERN OF ASDE-3 ANTENNA FEED HORN

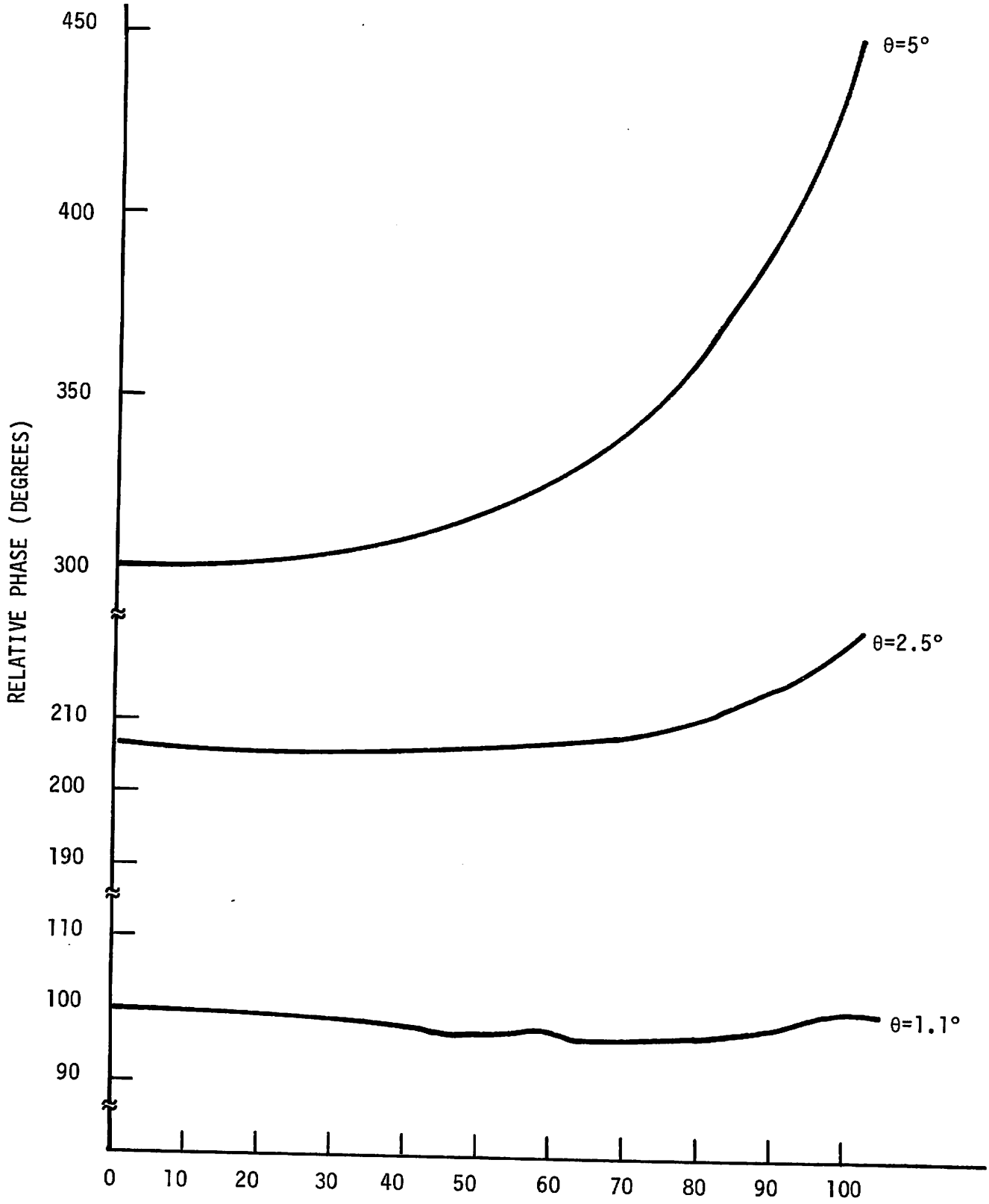

FIGURE 9. PHASE RUN-OFF ACROSS APERTURE

4. DESCRIPTION OF THE ROTODOME

The first ASDE-3 antenna was designed and built by Microwave Specialties Corp (MSC) of San Diego, CA. MSC also built the female master mold from which subsequent secondary molds were made in order to fabricate the reflector. The radome was designed by Teledyne Micronetics (T.M.) of San Diego, CA and fabricated by KDI Composite Technology, Inc., of Van Nuys, CA. TM integrated the two components and tested the complete assembly (rotodome) on their antenna range. Upon completion of the tests, it was shipped to Cardion Electronics in Long Island, NY, where it was accidently destroyed by fire.

A second rotodome was built with T.M. again assuming the responsibility for integration and test. Since the master mold was still available and the reflector design had been verified by computer analyses, T.M. contracted out the fabrication of the reflector to Performance Plastics of San Diego, CA and the rotodome to KDI.

The master mold was retrieved from MSC in order to be refurbished. During the repair, it was determined that the aluminum ribs used for establishing the contour had been incorrectly assembled. This error was corrected and the mold was completely rebuilt.

In addition to the reflector mold, slight modifications were made in the radome mold. The overall height was increased to allow for tilting the reflector and feed when adjusting for different tower heights.

The rotodome was assembled and tested at T.M. It was then disassembled and then shipped directly to FAATC where it was reassembled and installed on the ASDE tower. Figures 10 through 15 show interior views of the assembled rotodome.

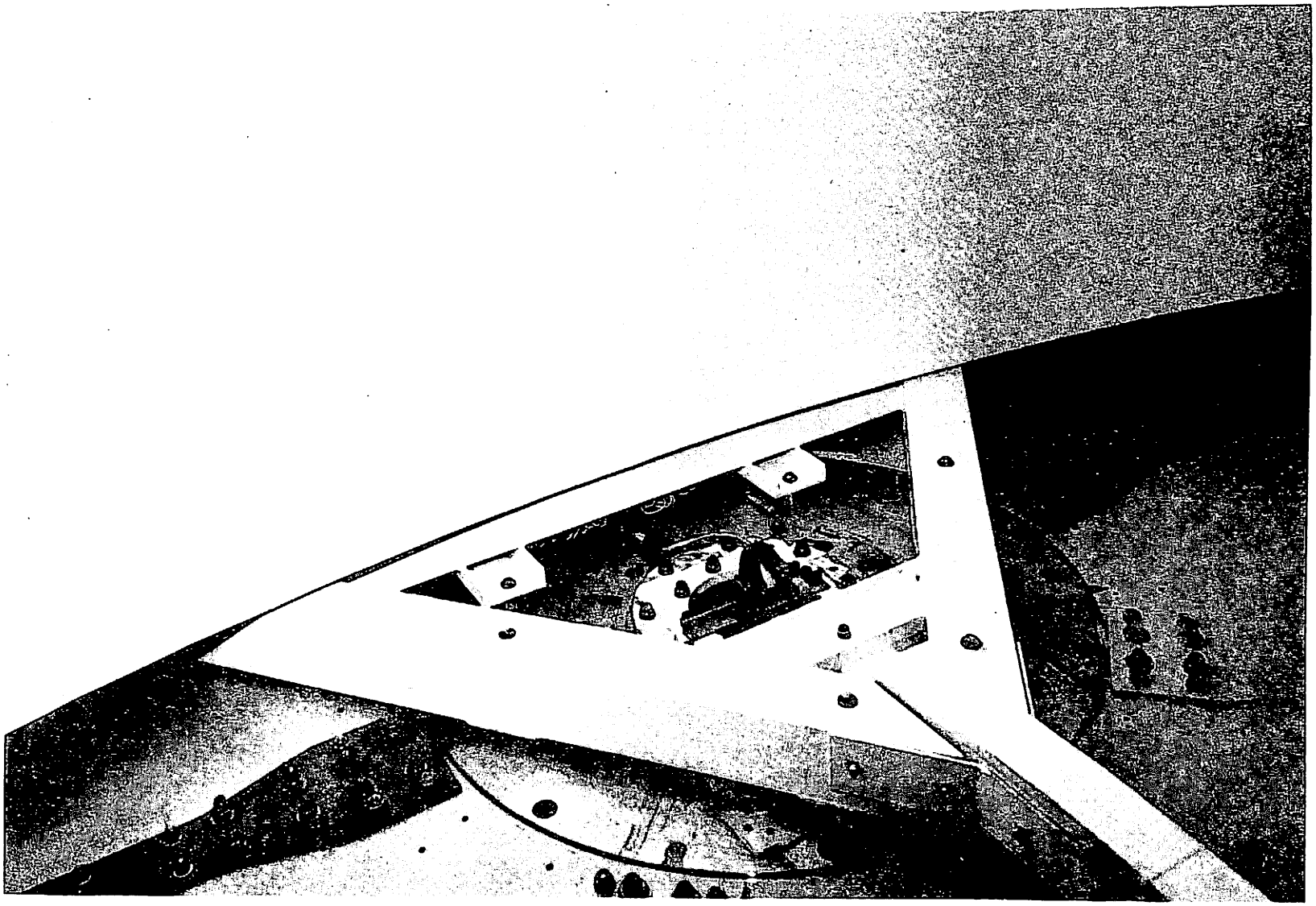

FIGURE 10. INTERIOR OF ROTODOME SHOWING WAVEGUIDE BEND AND REFLECTOR SUPPORT STRUCTURE

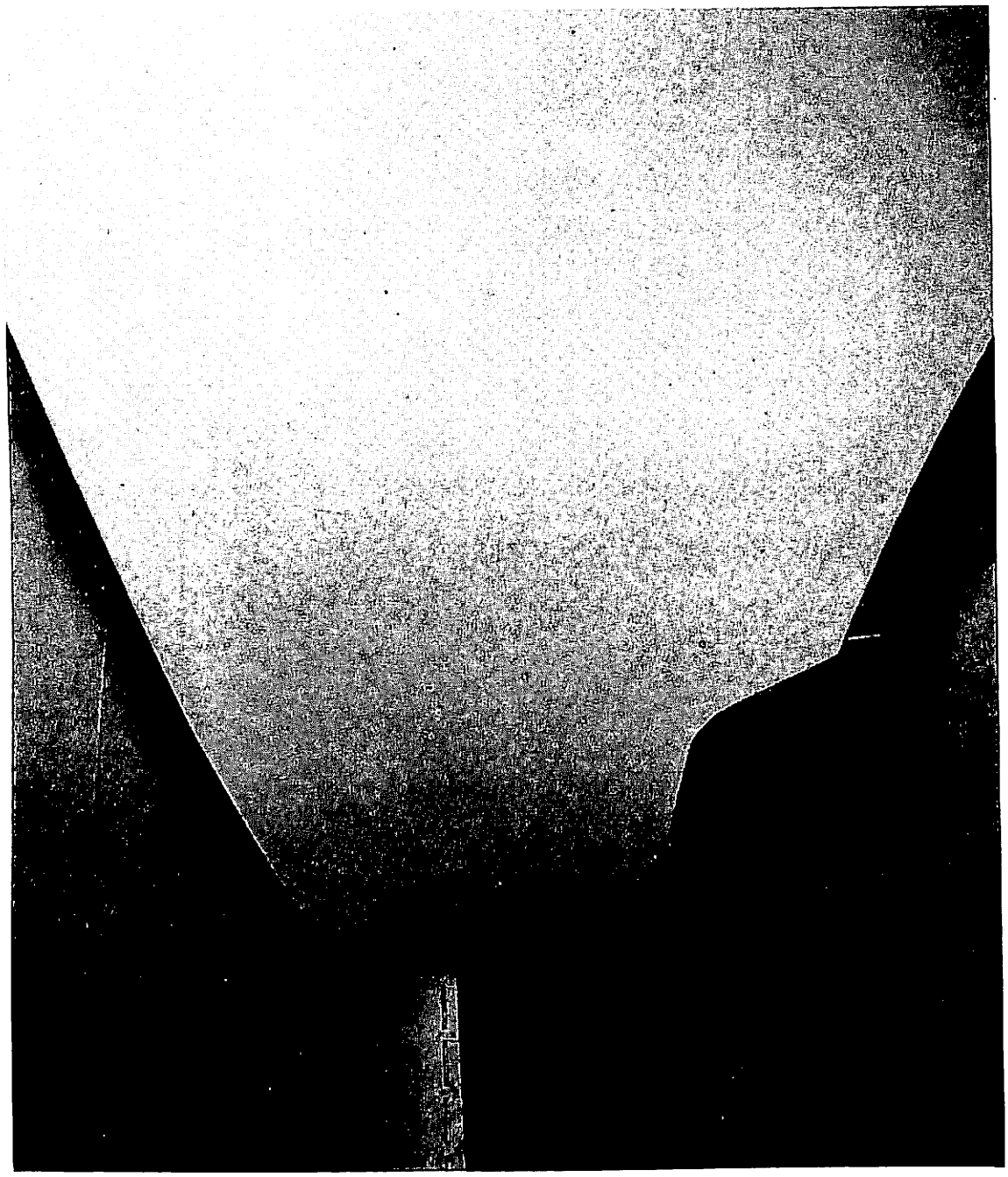

FIGURE 11. INTERIOR OF ROTODOME SHOWING REFLECTOR CUT-OUT TO ALLOW CIRCULATION OF HEATER AIR

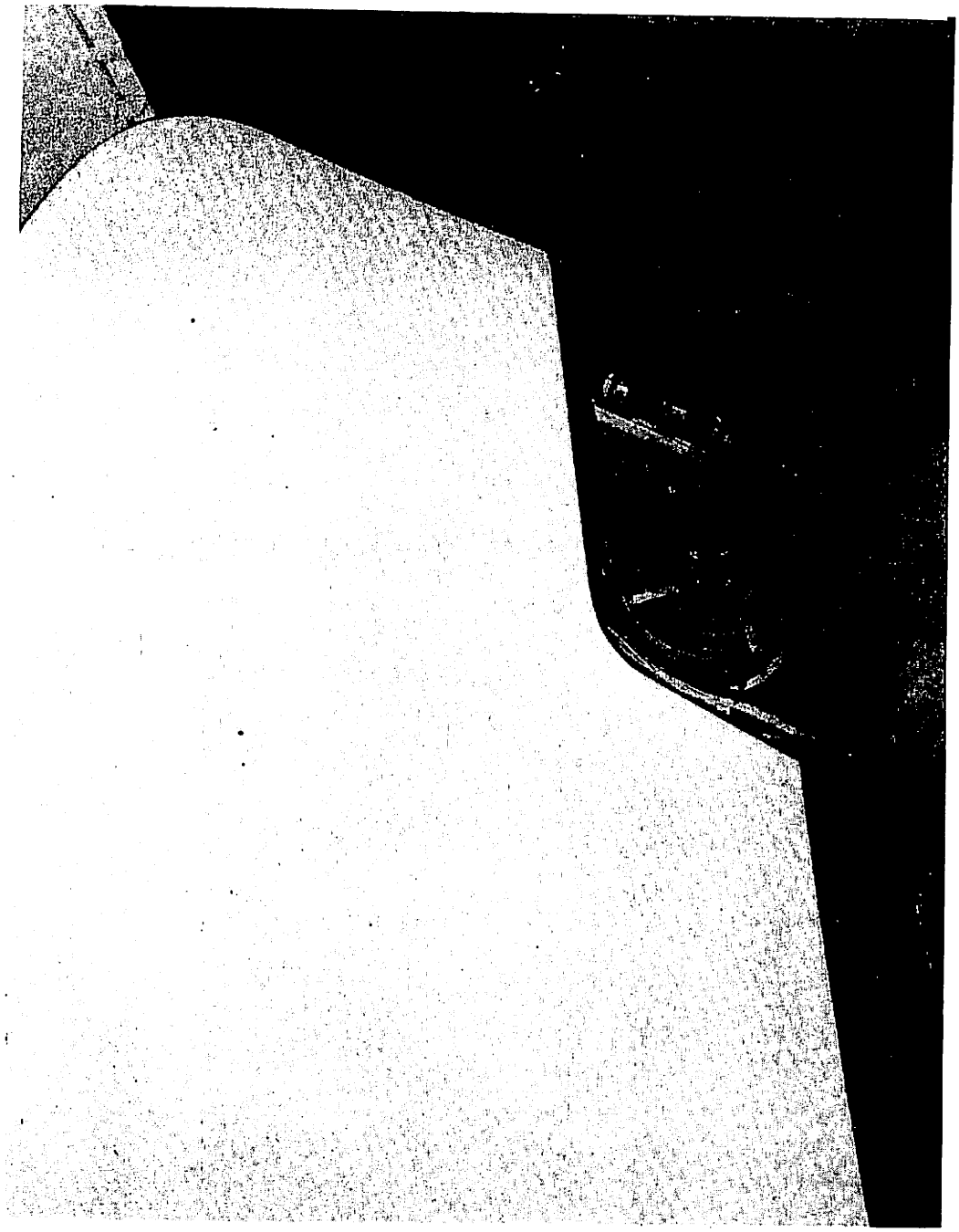

FIGURE 12. INTERIOR OF ROTODOME SHOWING ONE OF THE HEATERS

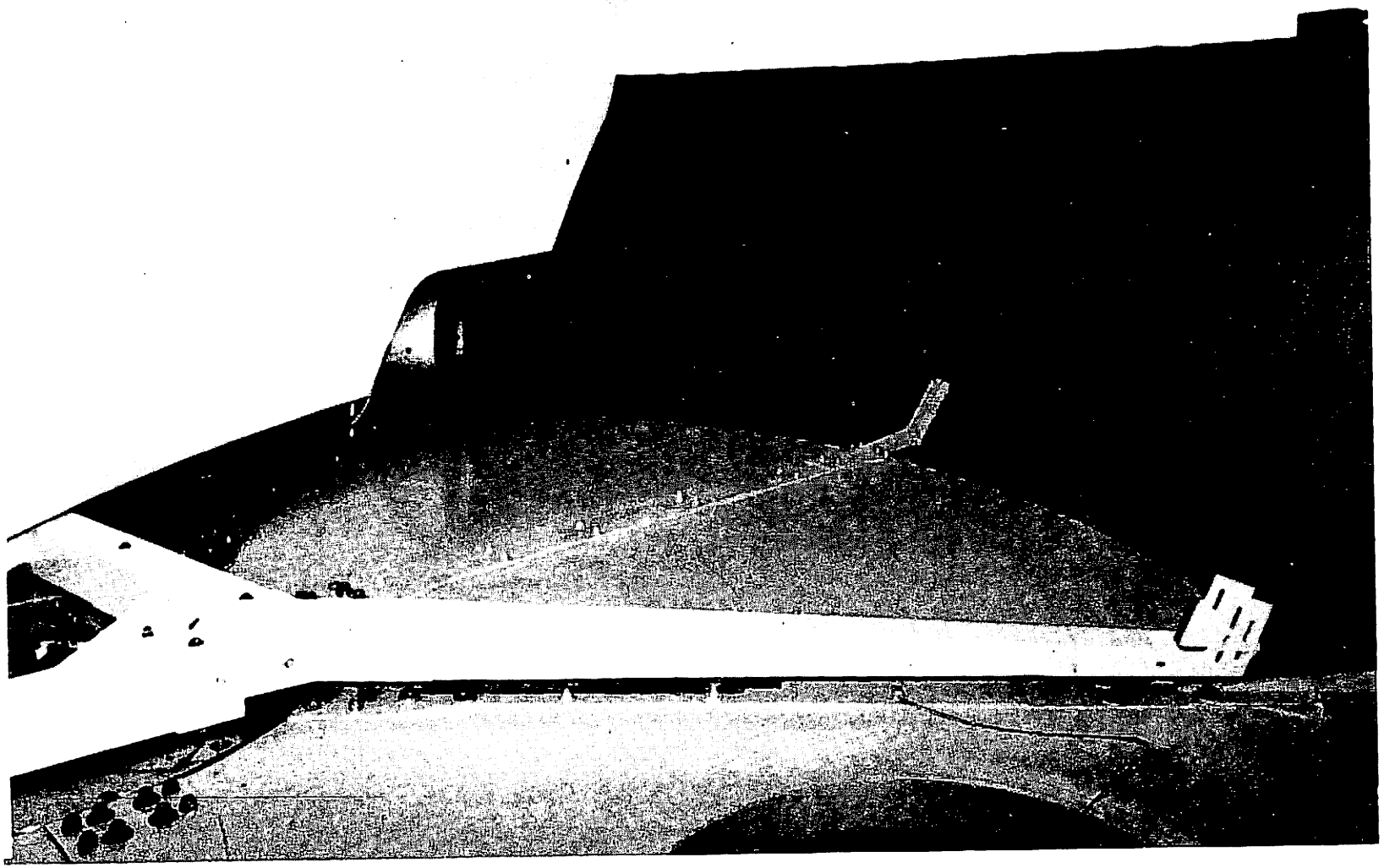

FIGURE 13. INTERIOR OF ROTODOME SHOWING HEATER AND FEED HORN ASSEMBLY

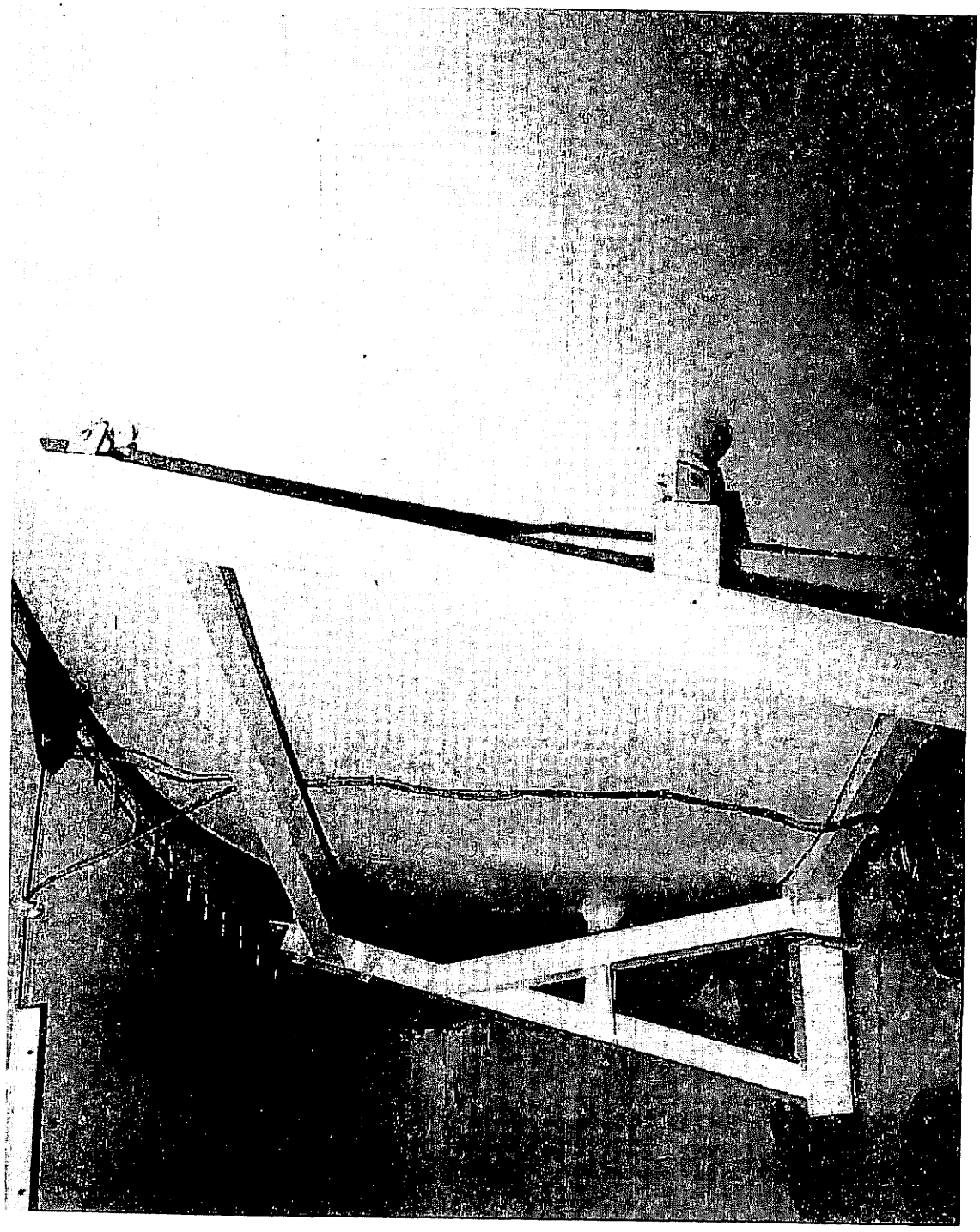

FIGURE 14. INTERIOR OF ROTODOME SHOWING BACK-SIDE OF REFLECTOR AND BACK-UP STRUCTURE

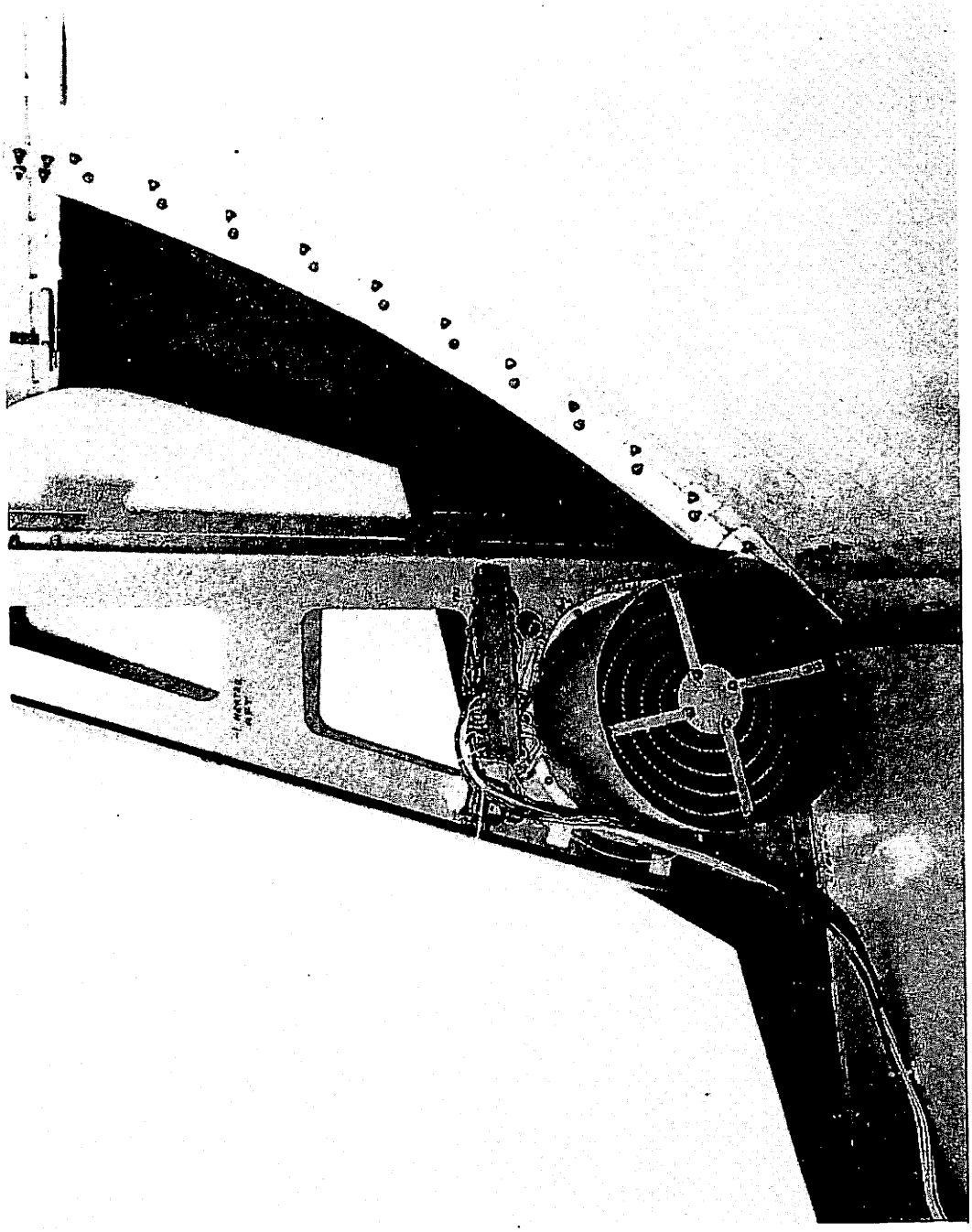

FIGURE 15. INTERIOR OF ROTODOME SHOWING HEATER AND REFLECTOR RESTRAINING BRACKETS

5. ANTENNA RANGE TEST

Static radiation pattern measurements were made by Teledyne Micronetics on their antenna range using two different distances between the transmitting antenna and the ASDE-3 antenna under test. A distance of 500 ft was used for the near-field measurements and 6800 ft for the far-field measurements. A limited number of azimuth and elevation patterns were taken of the antenna outside of the radome. The azimuth pattern data was compared with the same data taken on the antenna inside the radome. The results are tabulated in Table 1 and as is indicated, the radome had little adverse effect on the antenna performance.

A more complete set of patterns was taken of the antenna inside the radome. Typical azimuth and elevation patterns are shown in Figures 16 through 27 and the azimuth data is summarized in Table 2. The circular polarization gain data given in the table was plotted on the specific elevation antenna pattern to determine how well the antenna met the specification. Figures 28 through 30 show these data and indicate that the rotodome comes very close to meeting the circularly polarized gain and elevation beam shape specification. In comparing these figures with the actual range of Figures 22 through 27, one finds that the respective shaped beam patterns do not agree. The reason for the discrepancy is the fact that the actual range elevation patterns were taken at a fixed range and hence are defocussed at the low depression angles for the near-field case and at the large depression angles for the far field patterns. Overlaying the respective near- and far-field elevation patterns shows the difference in gain at these two extremes due to defocussing. Lack of time did not permit a more thorough experimental investigation of the depth of field and the defocussing effects of this antenna.

TABLE 1. EFFECT OF RADOME ON ASDE-3 ANTENNA RADIATION CHARACTERISTICS

MEASURED RADIATION CHARACTERISTICS OF ASDE-3 ANTENNA

	FREQ (GHz)	3dB BW	SLL (dB)	AXIAL RATIO (dB)	GAIN @ PEAK (dBic)	GAIN @ -20.5 (dBic)
Far Field	15.7 (w/o Radome)	0.25°	-19	1.0	44.7	
	15.7 (w/Radome)	0.27°	-20	0.5	45.0	
	15.95 (w/o Radome)	0.25°	-22	2.3	43.7	
	15.95 (w/Radome)	0.27°	-20	2.0	44.5	
	16.2 (w/o Radome)	0.25°	-19	3.0	44.7	
	16.2 (w/Radome)	0.24°	-17	3.0	44	
Near Field	15.7 (w/o Radome)	0.30°	-17	1		30
	15.7 (w/Radome)	0.30°	-16	1		29
	15.95 (w/o Radome)	0.31°	-16	1.5		31.5
	15.95 (w/Radome)	0.30°	-17	1.5		31.5
	16.2 (w/o Radome)	0.31°	-18	2.5		30.7
	16.2 (w/Radome)	0.28°	-17	3.0		30.4

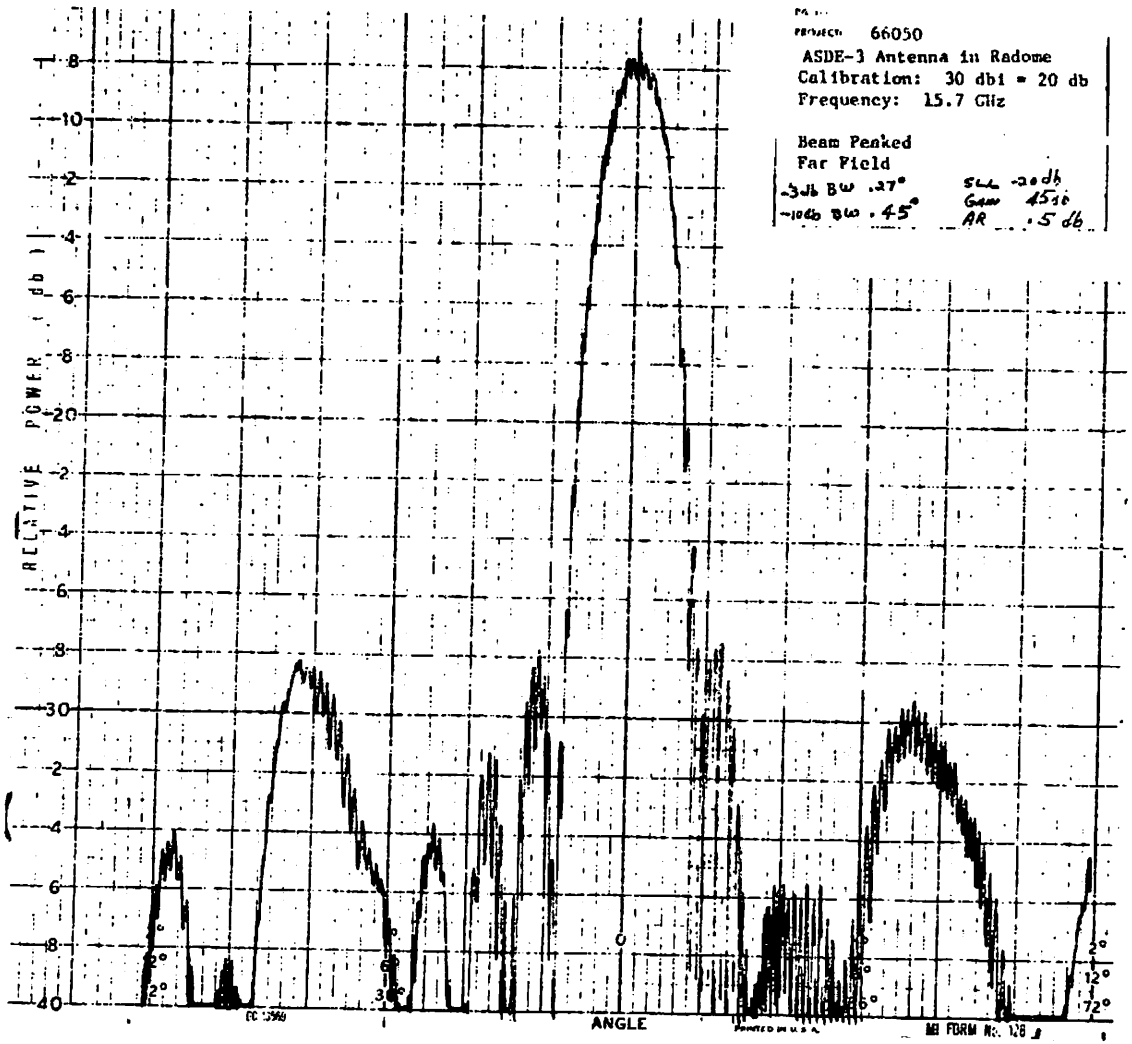

FIGURE 16. ASDE-3 ANTENNA AZIMUTH RADIATION PATTERN (Farfield, 15.7 GHz)

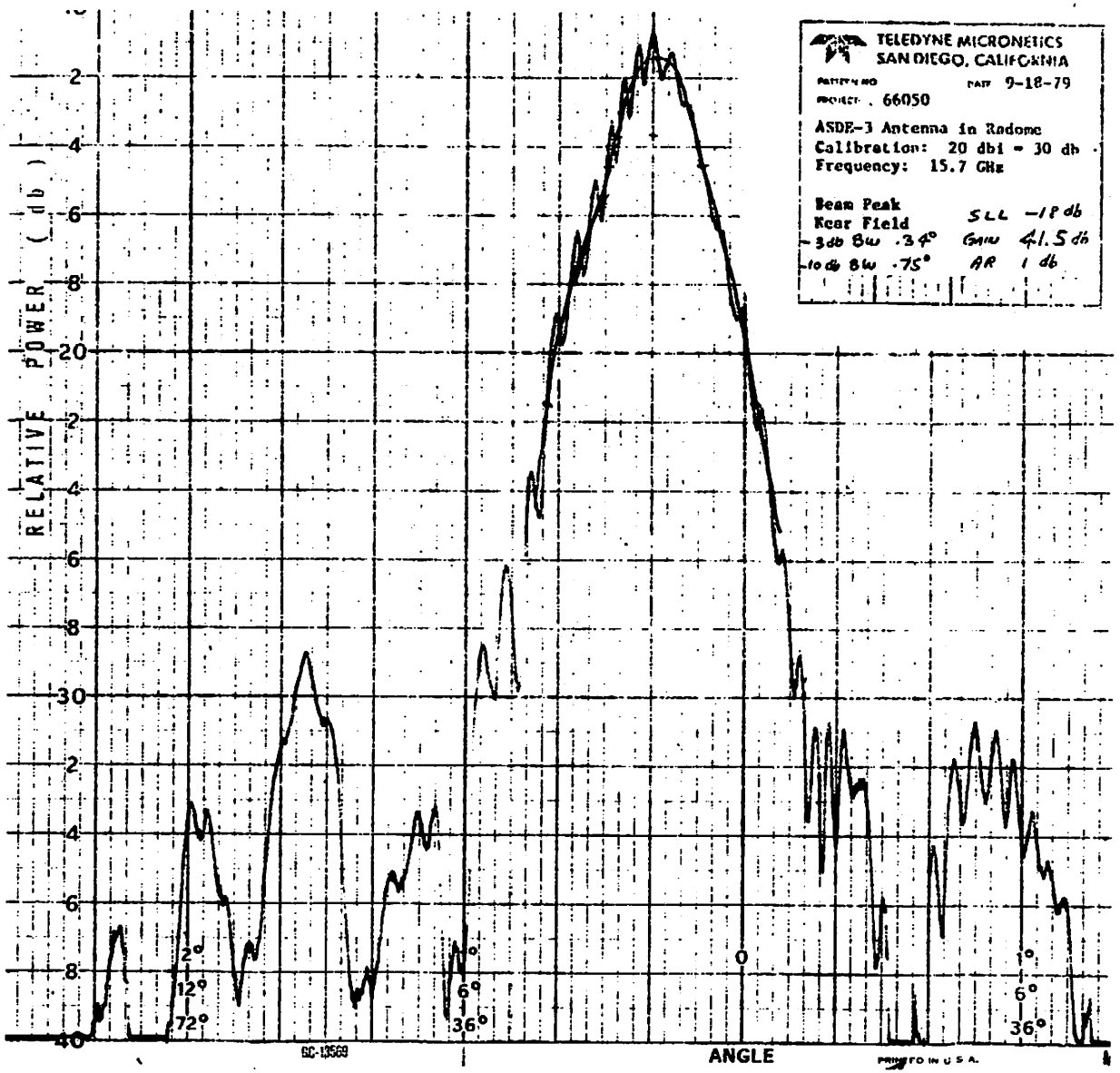

FIGURE 17. ASDE-3 ANTENNA AZIMUTH RADIATION PATTERN (Nearfield, 15.7 GHz)

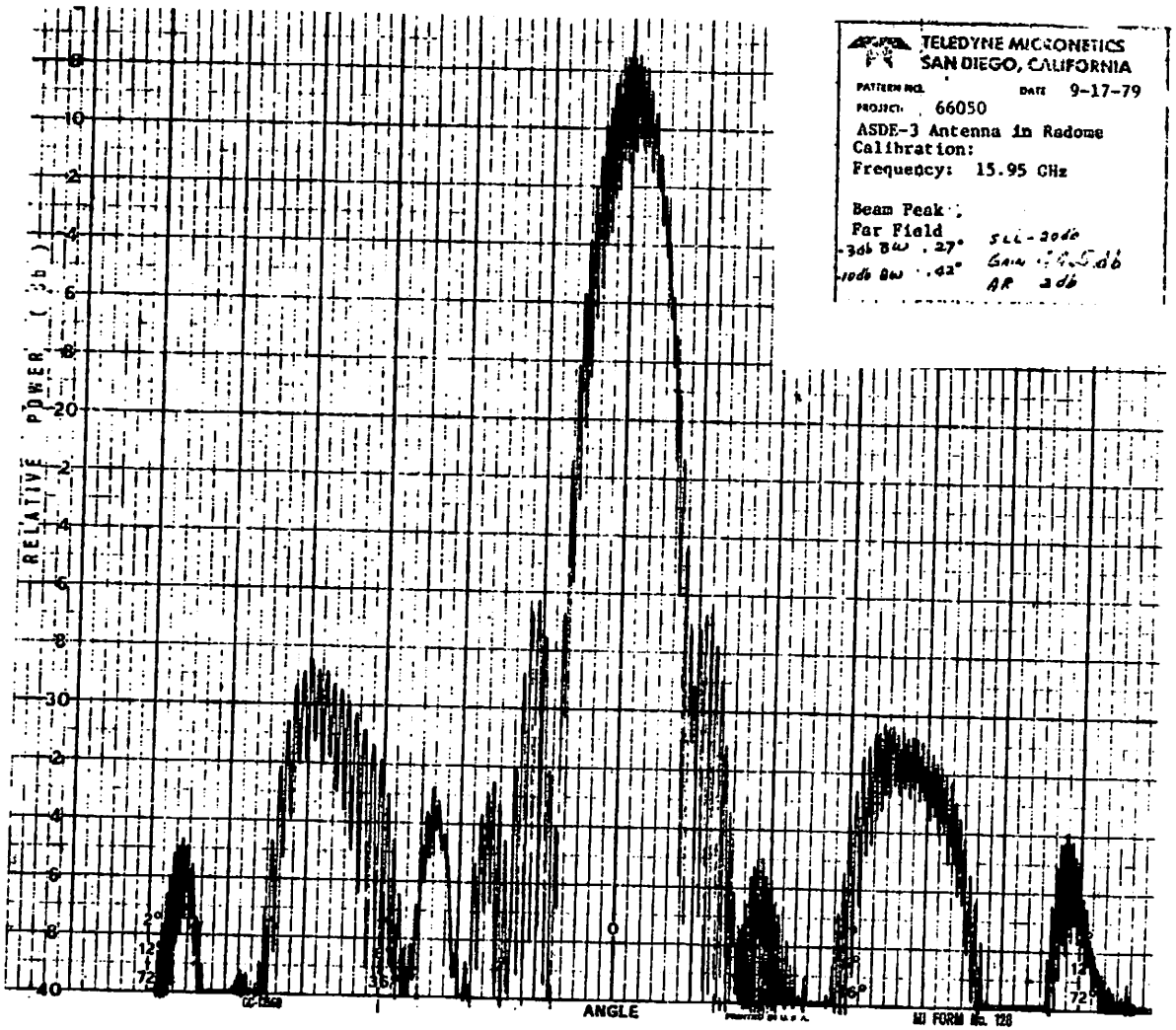

FIGURE 18. ASDE-3 ANTENNA AZIMUTH RADIATION PATTERN (Farfield, 15.95 GHz)

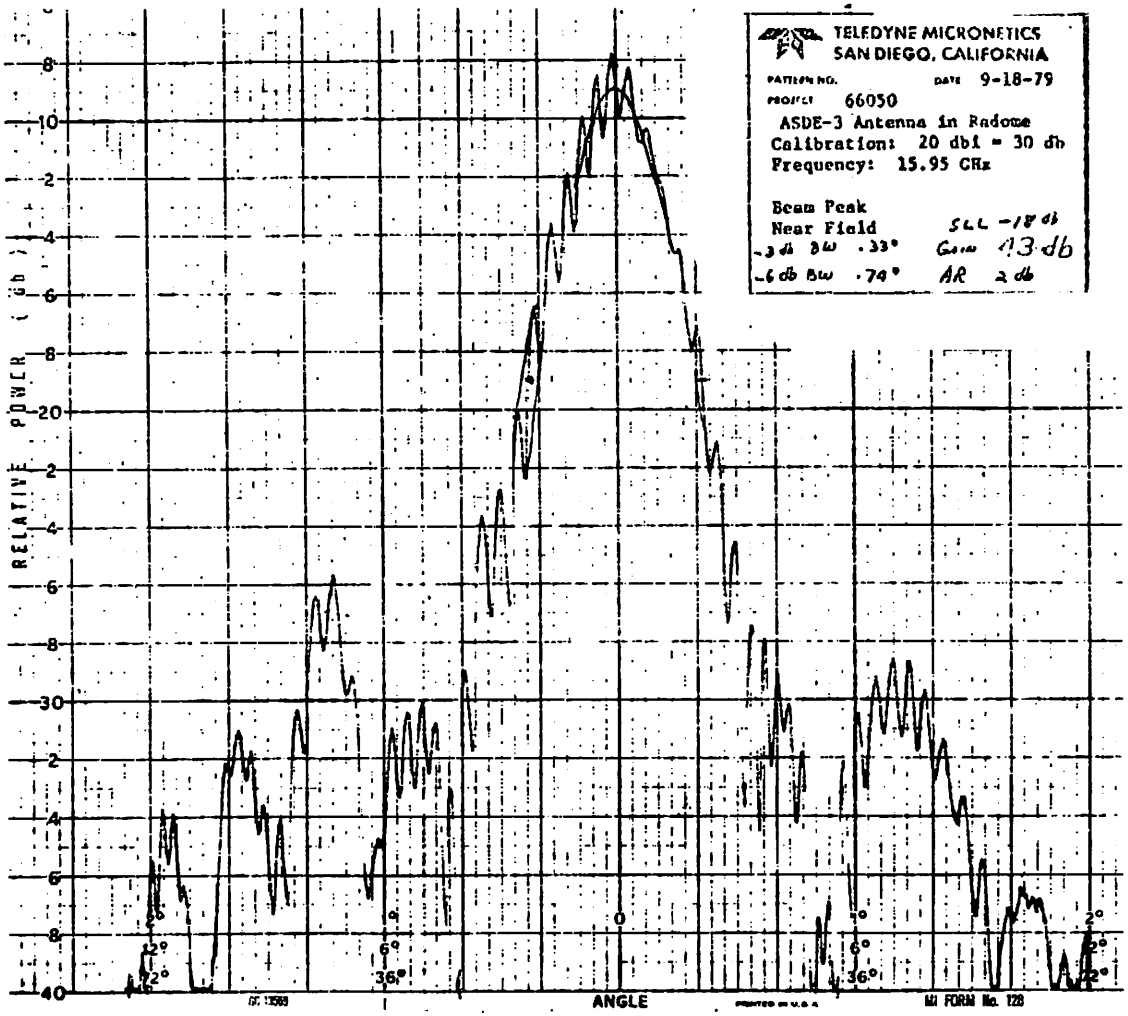

FIGURE 19. ASDE-3 ANTENNA AZIMUTH RADIATION PATTERN (Nearfield, 15.95 GHz)

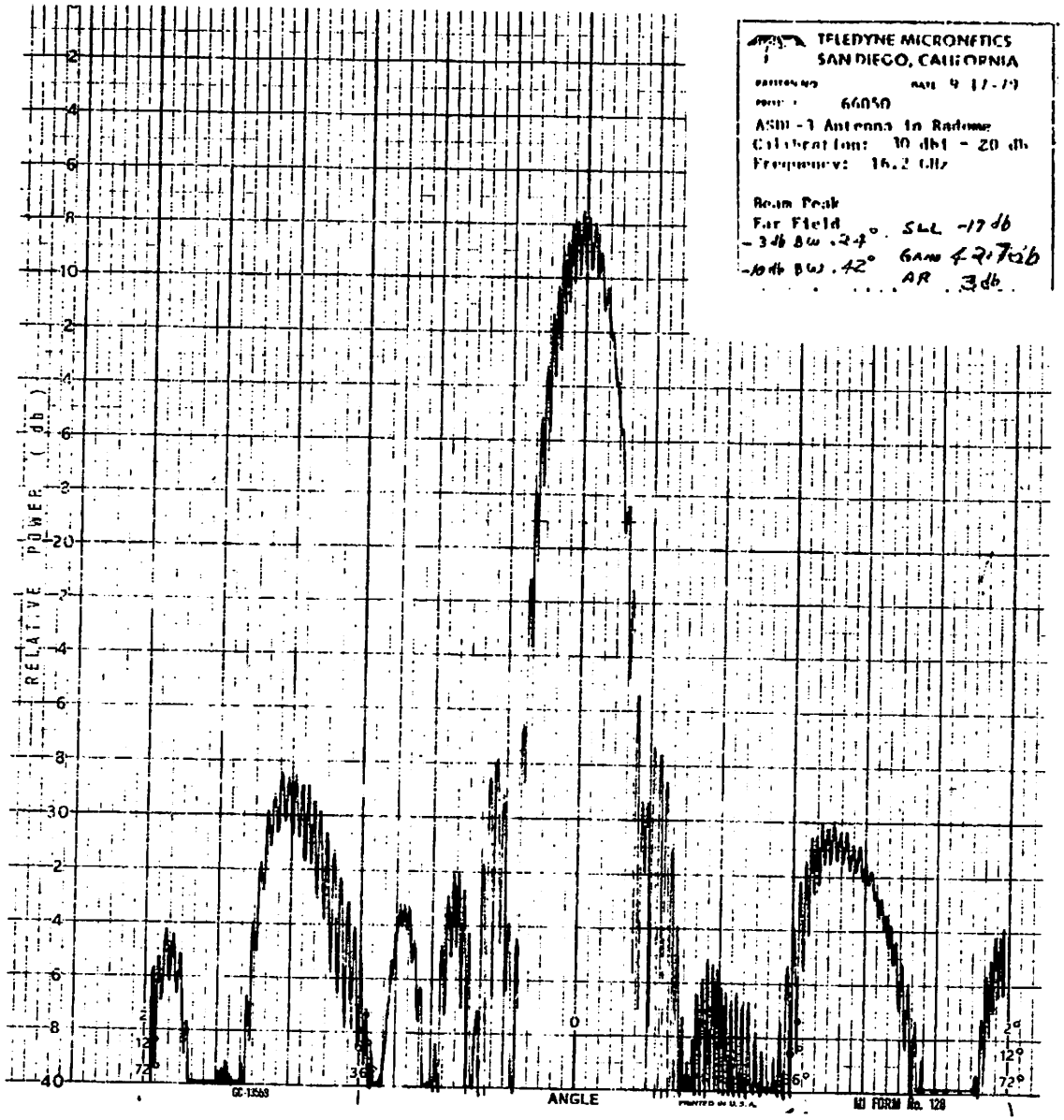

FIGURE 20. ASDE-3 ANTENNA AZIMUTH RADIATION PATTERN (Farfield, 16.2 GHz)

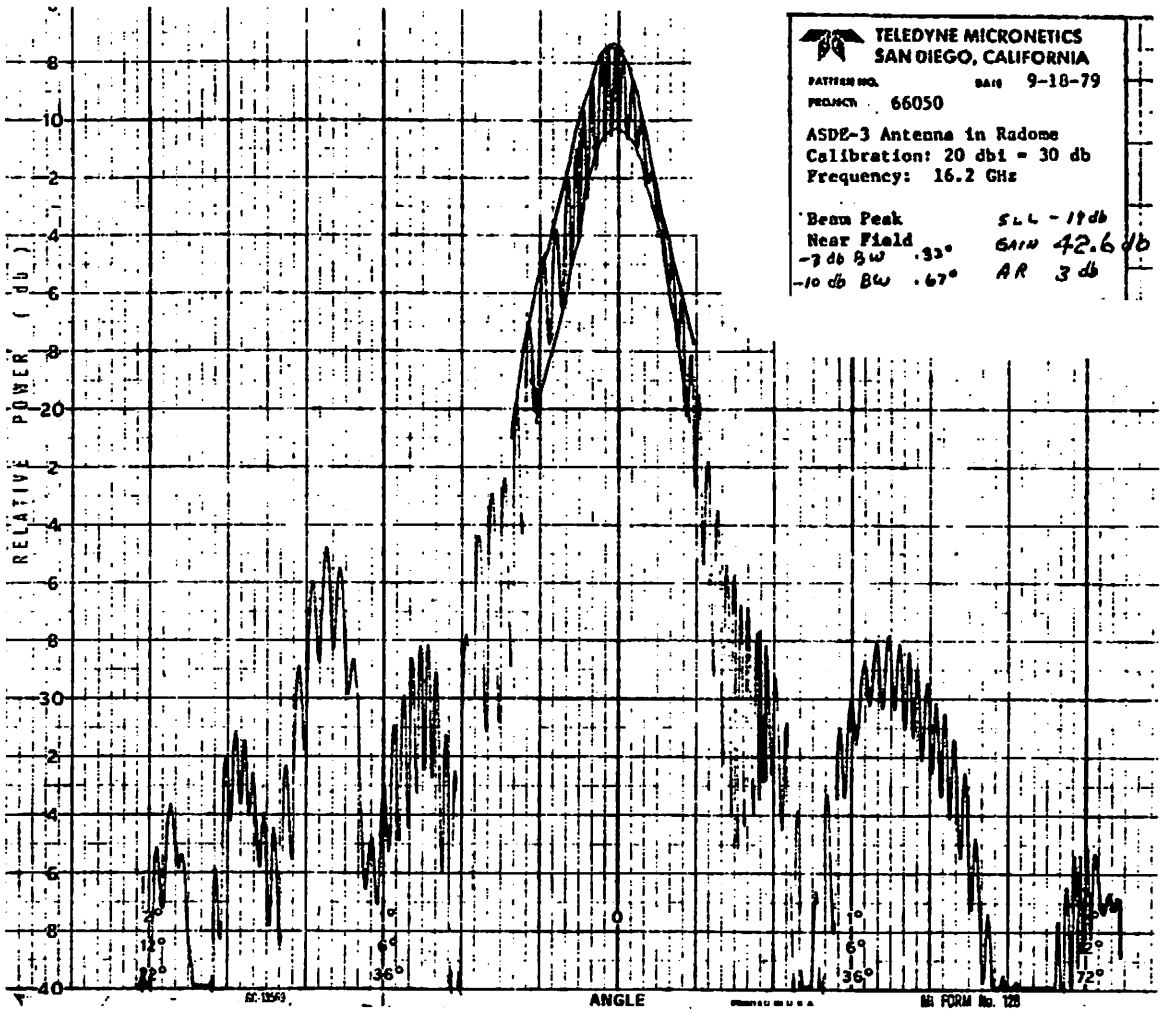

FIGURE 21. ASDE-3 ANTENNA AZIMUTH RADIATION PATTERN (Nearfield, 16.2 GHz)

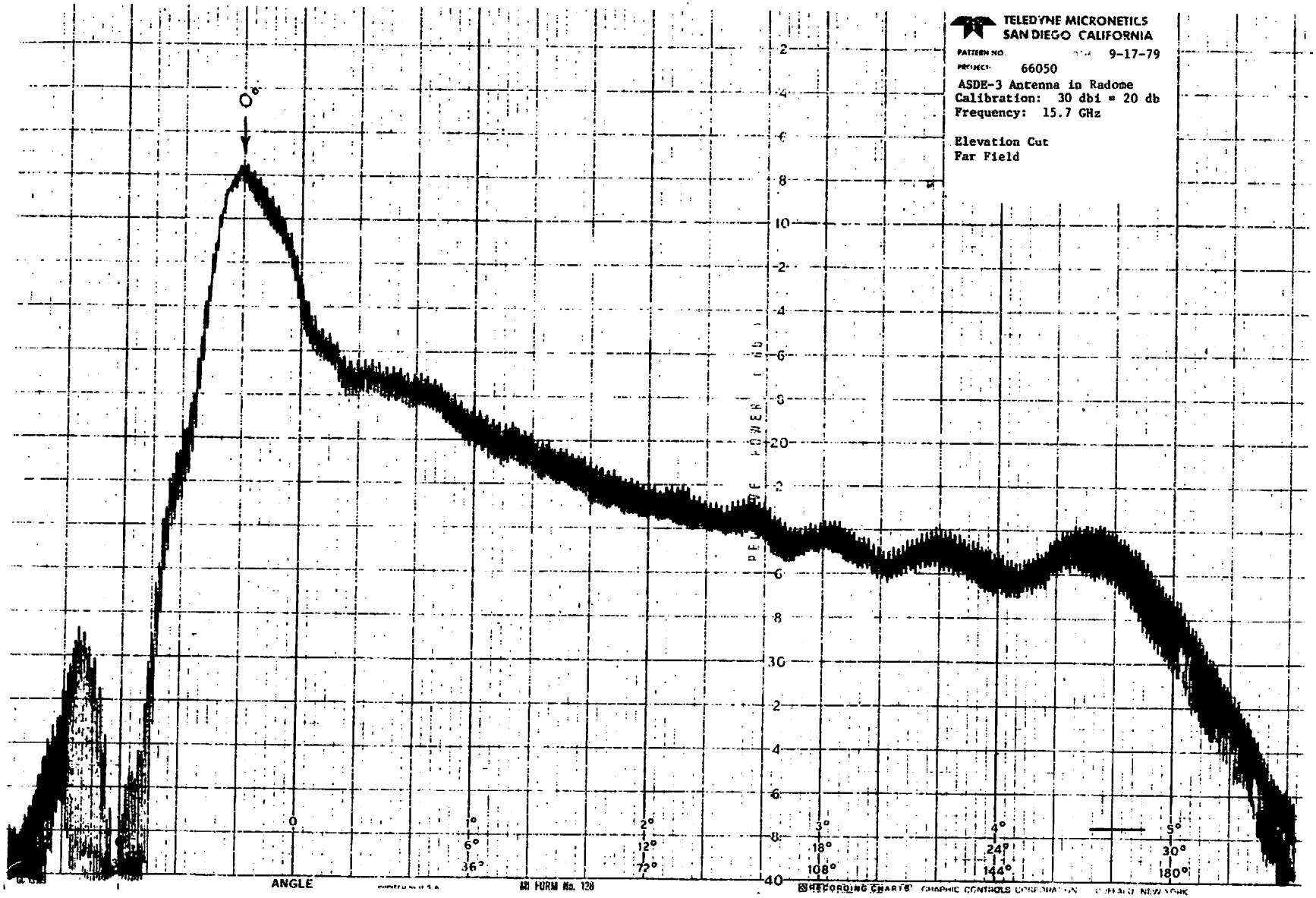

FIGURE 22. ASDE-3 ANTENNA ELEVATION RADIATION PATTERN (Farfield, 15.7 GHz)

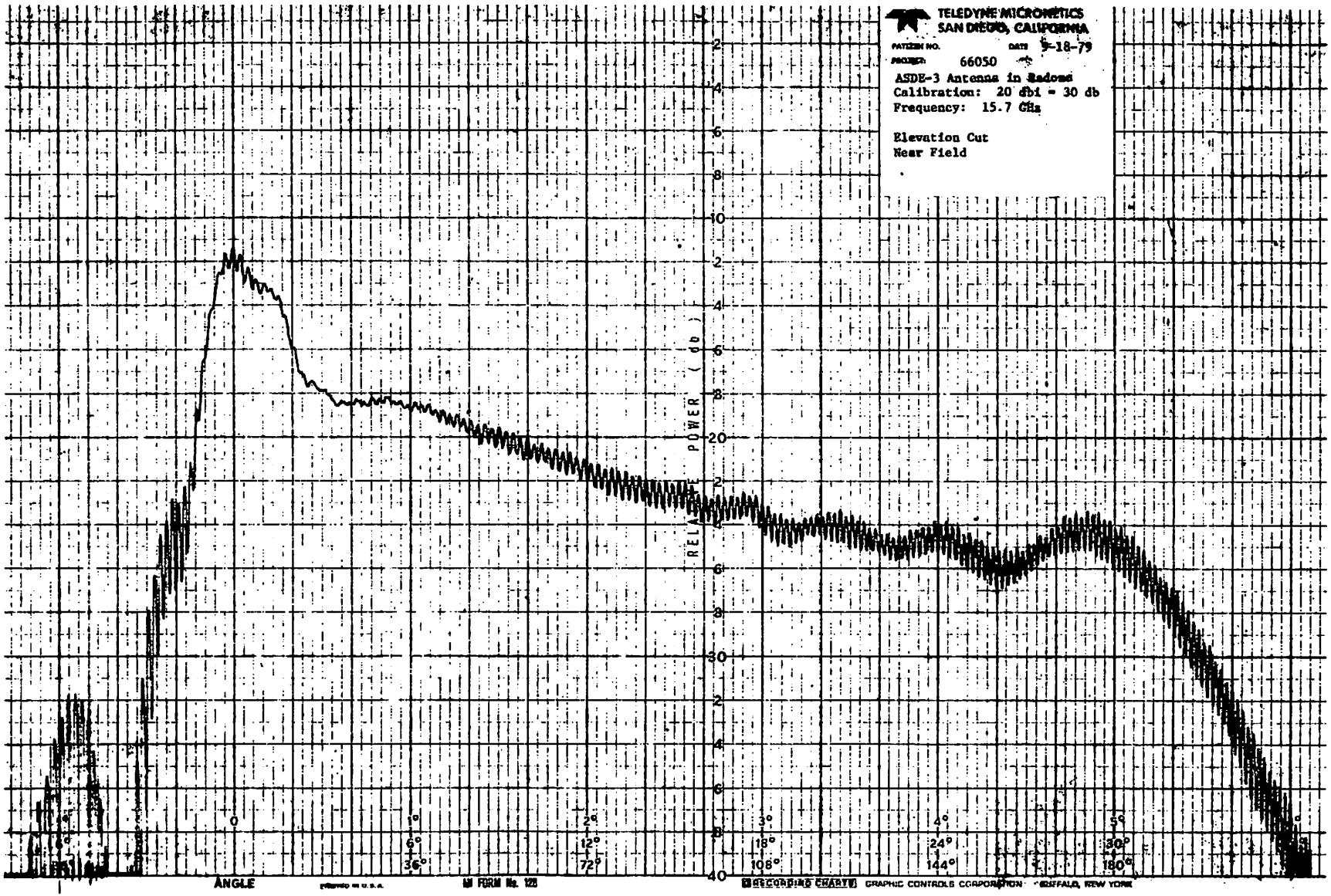

FIGURE 23. ASDE-3 ANTENNA ELEVATION RADIATION PATTERN (Nearfield, 15.7 GHz)

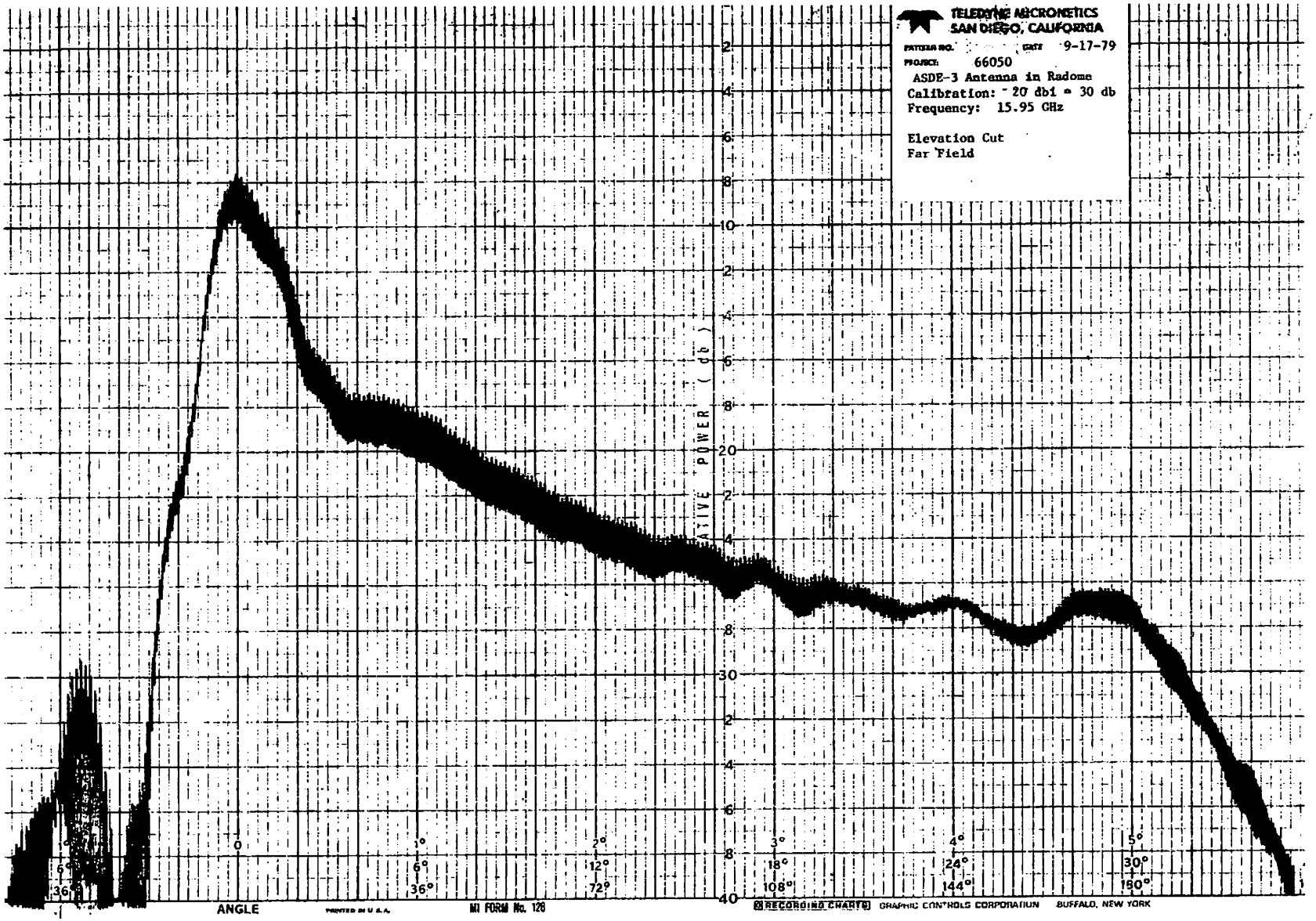

FIGURE 24. ASDE-3 ANTENNA ELEVATION RADIATION PATTERN (Farfield, 15.95 GHz)

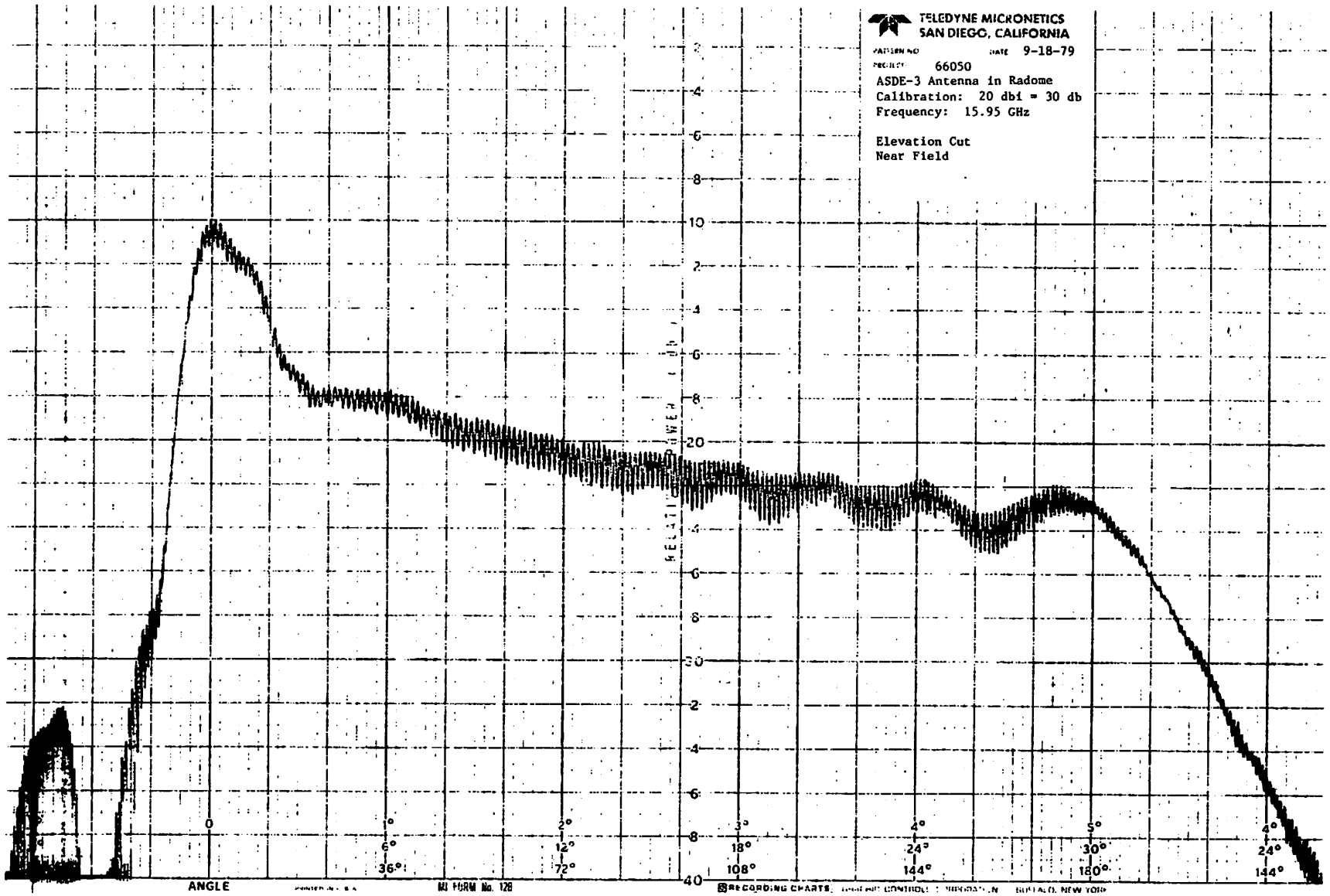

FIGURE 25. ASDE-3 ANTENNA ELEVATION RADIATION PATTERN (Nearfield, 15.95 GHz)

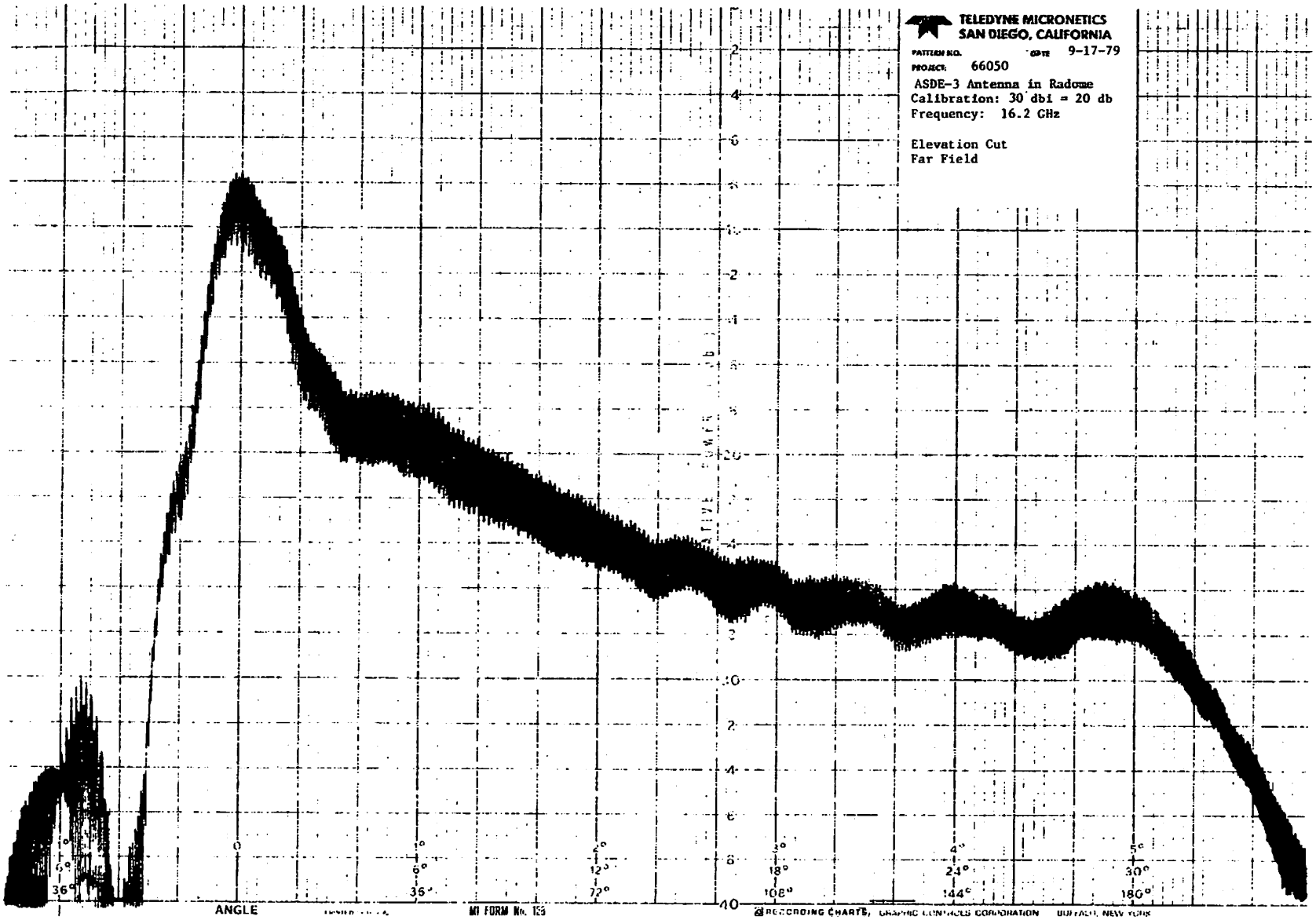

FIGURE 26. ASDE-3 ANTENNA ELEVATION RADIATION PATTERN (Farfield, 16.2 GHz)

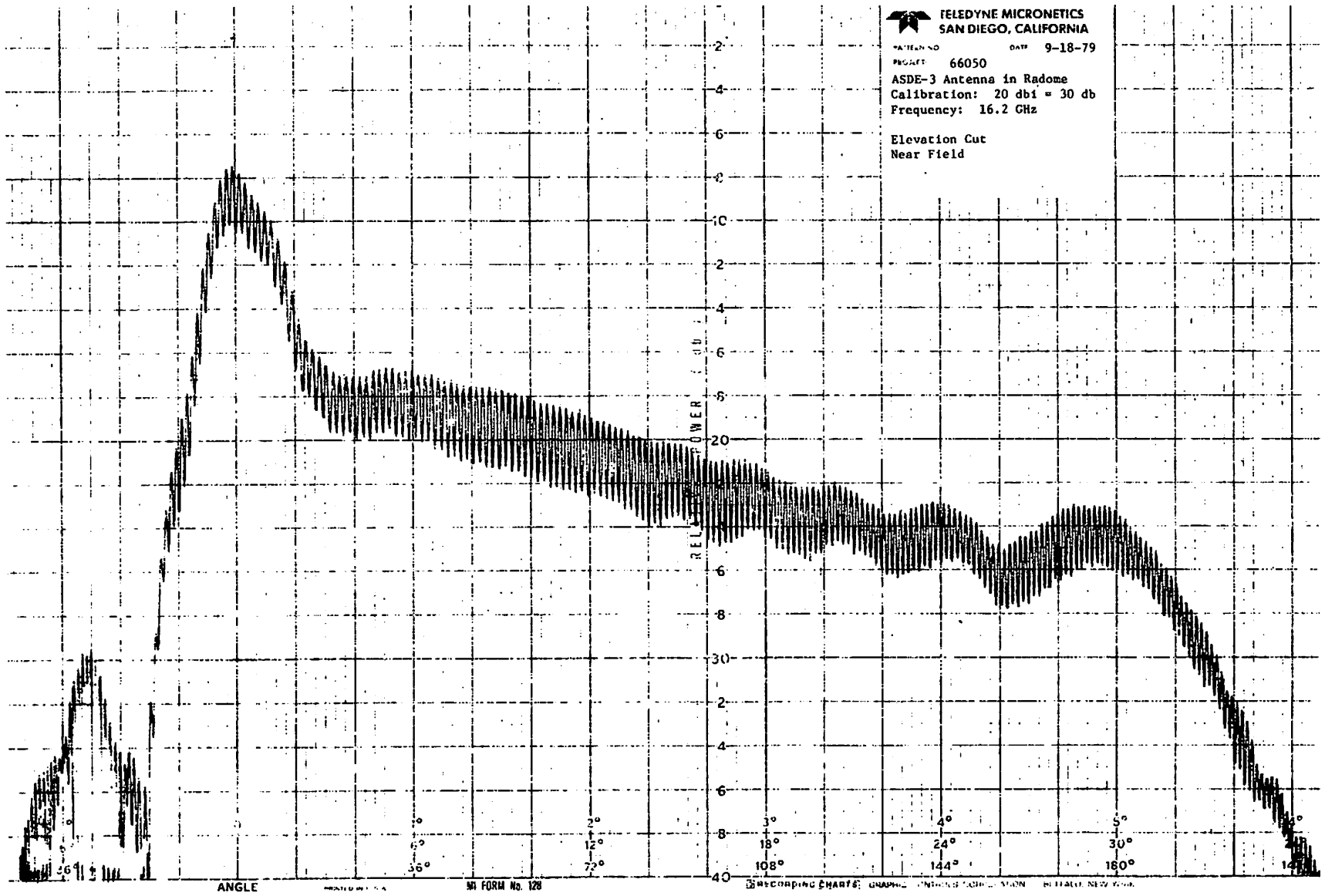

FIGURE 27. ASDE-3 ANTENNA ELEVATION RADIATION PATTERN (Nearfield, 16.2 GHz)

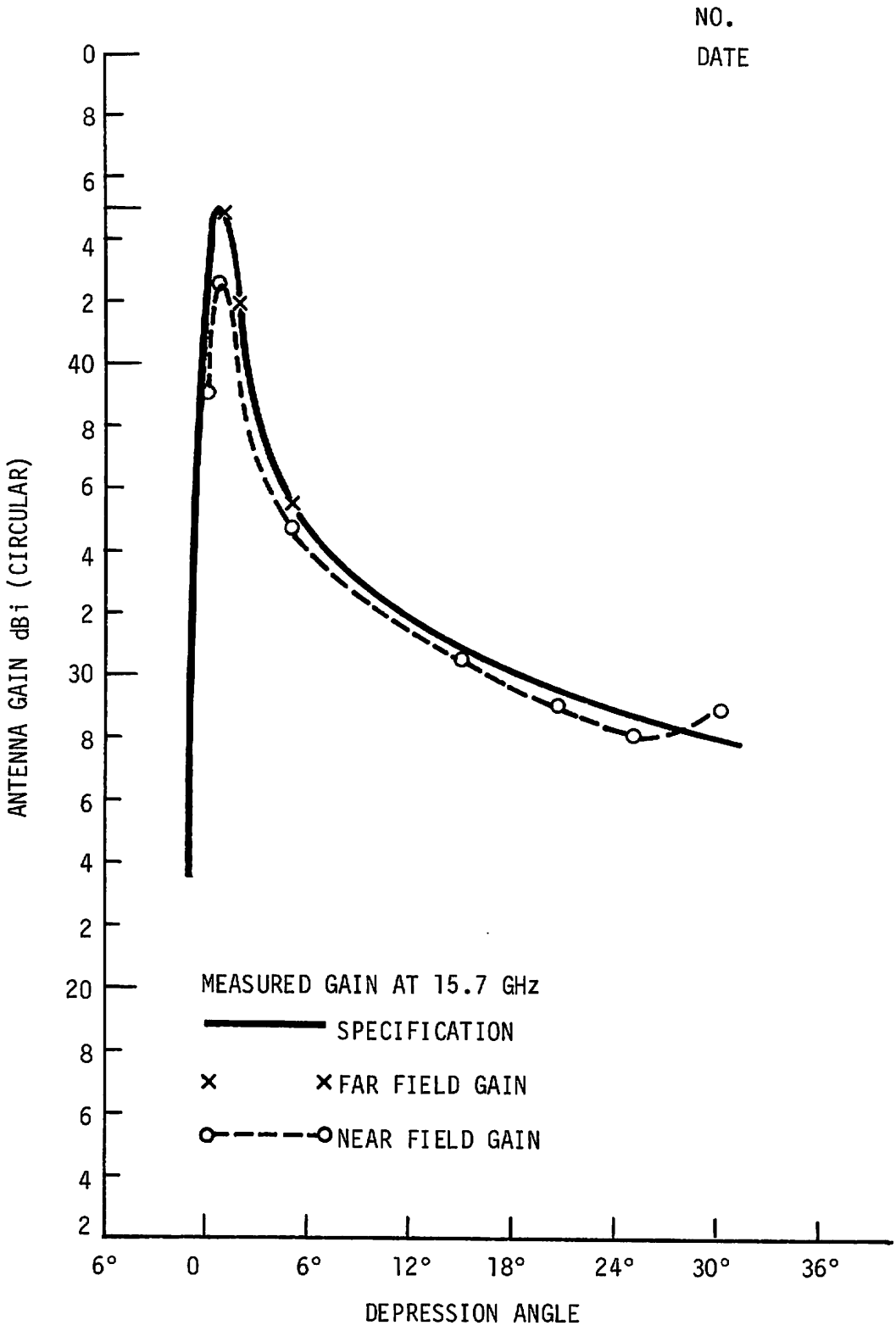

FIGURE 28. SUMMARY OF TELEDYNE MICRONETICS RANGE DATA @ 15.7 GHz

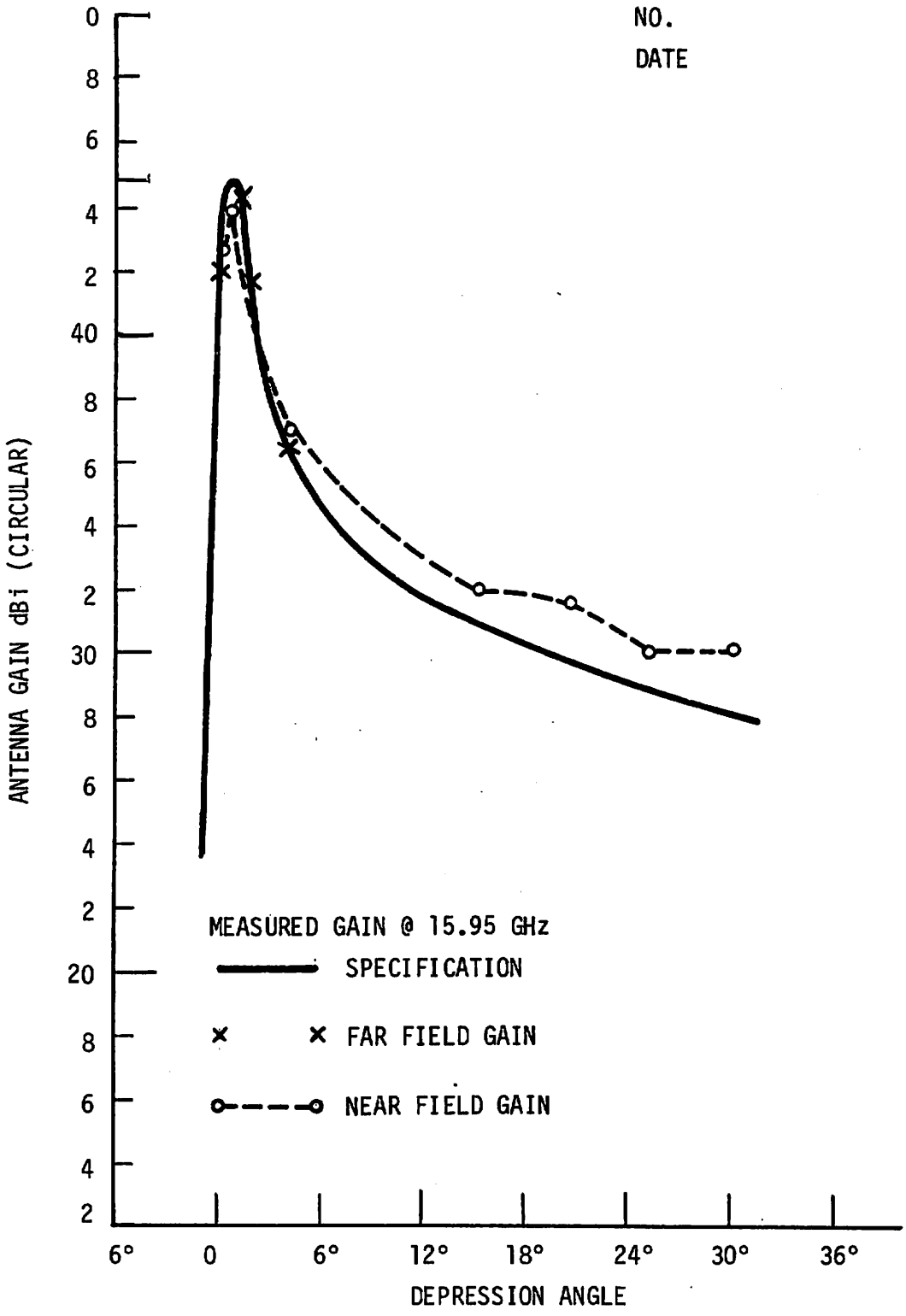

FIGURE 29. SUMMARY OF TELEDYNE MICRONETICS RANGE DATA @ 15.95 GHz

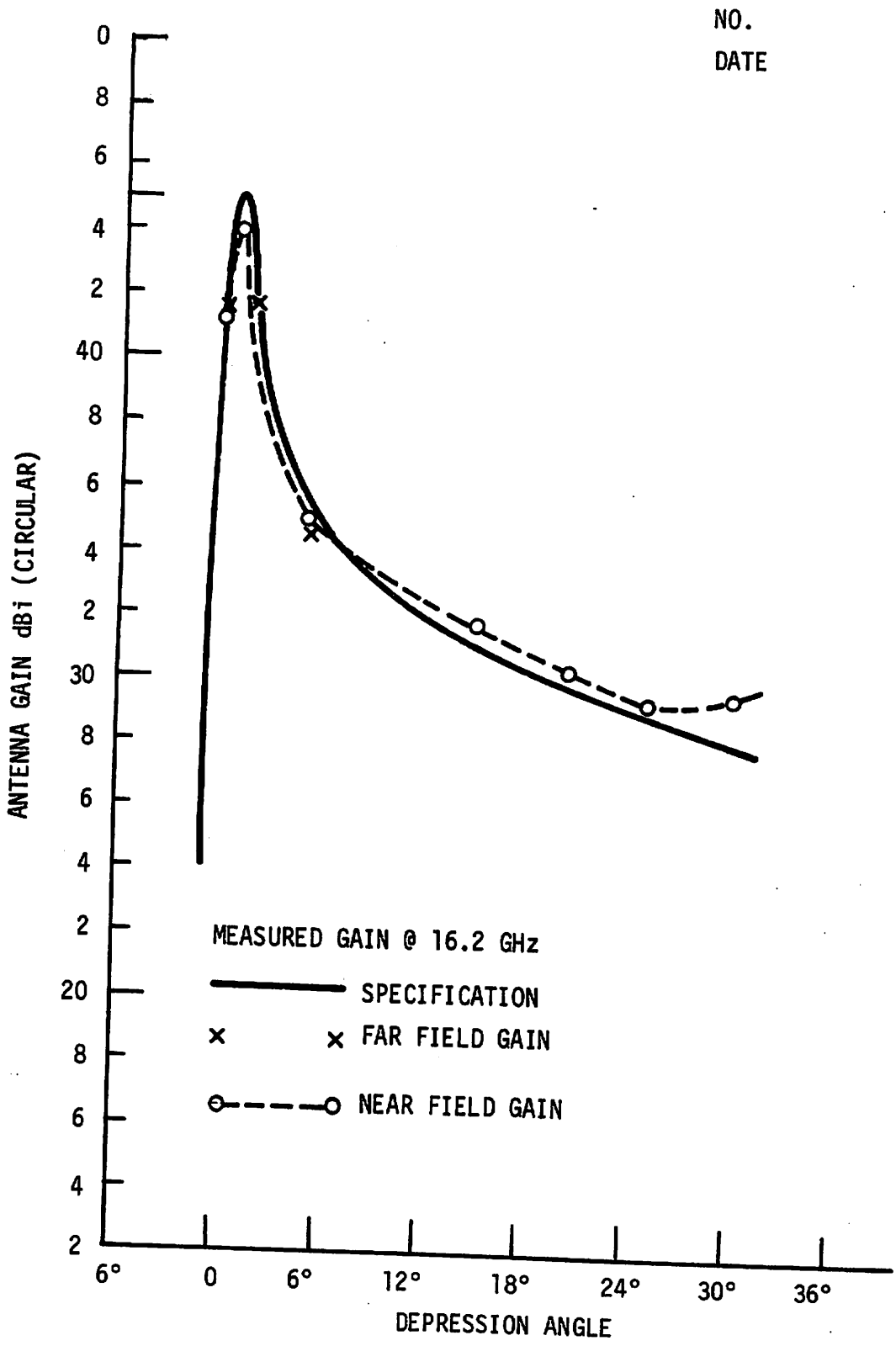

FIGURE 30. SUMMARY OF TELEDYNE MICRONETICS RANGE DATA @ 16.2 GHz

TABLE 2. SUMMARY OF TELEDYNE MICRONETICS RANGE DATA ON ASDE-3 ROTODOME

		NEAR FIELD				FAR FIELD			
FREQ (GHz)	DEPRESSION ANGLE	3 db BW	SLL (dB)	AXIAL RATIO (dB)	GAIN dBic	3 dB BW	SLL (dB)	AXIAL RATIO (dB)	GAIN dBic
15.7	Beam Peak	0.34°	-18	1.0	41.5	0.27°	-20	0.5	45
	Upper 3dB	0.28°	-21	0.5	39.0	0.27°	-16	1.0	41.5
	5°	0.28°	-21	0	34.7	0.30°	-20	1.0	35.5
	15°	0.28°	-17	1.0	30.5				
	20.5°	0.30°	-16	1.0	29				
	25°	0.37°	-12	1.0	28				
	30°	0.38°	-10	1.0	28.8				
15.95	Beam Peak	0.33°	-18	2.0	44	0.27°	-20	2.0	44.5
	Upper 3dB	0.30°	-21	1.5	42.8	0.27°	-17	1.0	42
	5°	0.28°	-20	1.0	36	0.27°	-21	2.0	34.5
	15°	0.28°	-15	2.0	32				
	20.5°	0.30°	-17	1.5	31.5				
	25°	0.30°	-13	1.0	30				
	30°	0.40°	-11	.5	30.2				
16.2	Beam Peak	0.33°	-19	3.0	44	0.24°	-17	3.0	44
	Upper 3dB	0.31°	-20	2.5	41.3	0.25°	-17	2.5	41.5
	5°	0.28°	-20	2.5	34.8	0.26°	-19	2.5	34.5
	15°	0.30°	-20	3.0	31.7				
	20.5°	0.28°	-17	3.0	30.3				
	25°	0.33°	-13	2.5	29.3				
	30°	0.42°	-10	2.5	29.4				

In addition to the static radiation patterns, dynamic radiation patterns were taken by Teledyne Micronetics, by observing the detected signal on an oscilloscope as the antenna was rotated at the specified 60 rpm. Their results showed little, if any, change between the static and dynamic azimuth radiation patterns. However, when dynamic tests were conducted at FAATC appreciable differences were observed. These results are discussed in Section 6.

6. DYNAMIC TESTS AT FAATC

6.1 DESCRIPTION OF TESTS

After the ASDE-3 radar installation and preliminary check-out had been completed, "in situ" dynamic tests of the rotodome were begun in order to verify antenna performance. The technique used was to transmit a CW signal from the airport surface to the rotating antenna on the tower. The ASDE-3 receiving subsystem receives, amplifies and detects this signal, which is then measured at the video output. As the rotodome rotates, the amplitude of this video signal varies in proportion to the rotodome azimuth pattern at the depression angle determined by the distance of the transmitting antenna from the tower. The antenna gain is determined by comparing the signal received from the rotodome with that received from a standard gain horn. Figures 31 through 33 show the standard gain horn installation and the waveguide switch which permits remote switching between the rotodome and standard gain horn. The radiation patterns are computed and plotted by the DAS, which samples the video output for each PRF, averages a number of corresponding PFR samples, computes dB levels and plots the azimuth pattern. Figure 34 shows the transmitting antenna and a view from Pad #1.

When these measurements were begun, however, the DAS was not available so that preliminary azimuth patterns had to be observed on an oscilloscope, whose horizontal sweep was triggered by the pedestal Azimuth Reference Pulses (ARP) through an adjustable delay, and whose sweep time could be adjusted to display the received signal vs. azimuth angle.

6.2 PRELIMINARY RESULTS

Since the DAS was not available at the time, preliminary rotodome check-out was accomplished by using the oscilloscope technique previously described in Section 6.1. Figures 35 through 37 are photographs of typical antenna azimuth patterns taken by

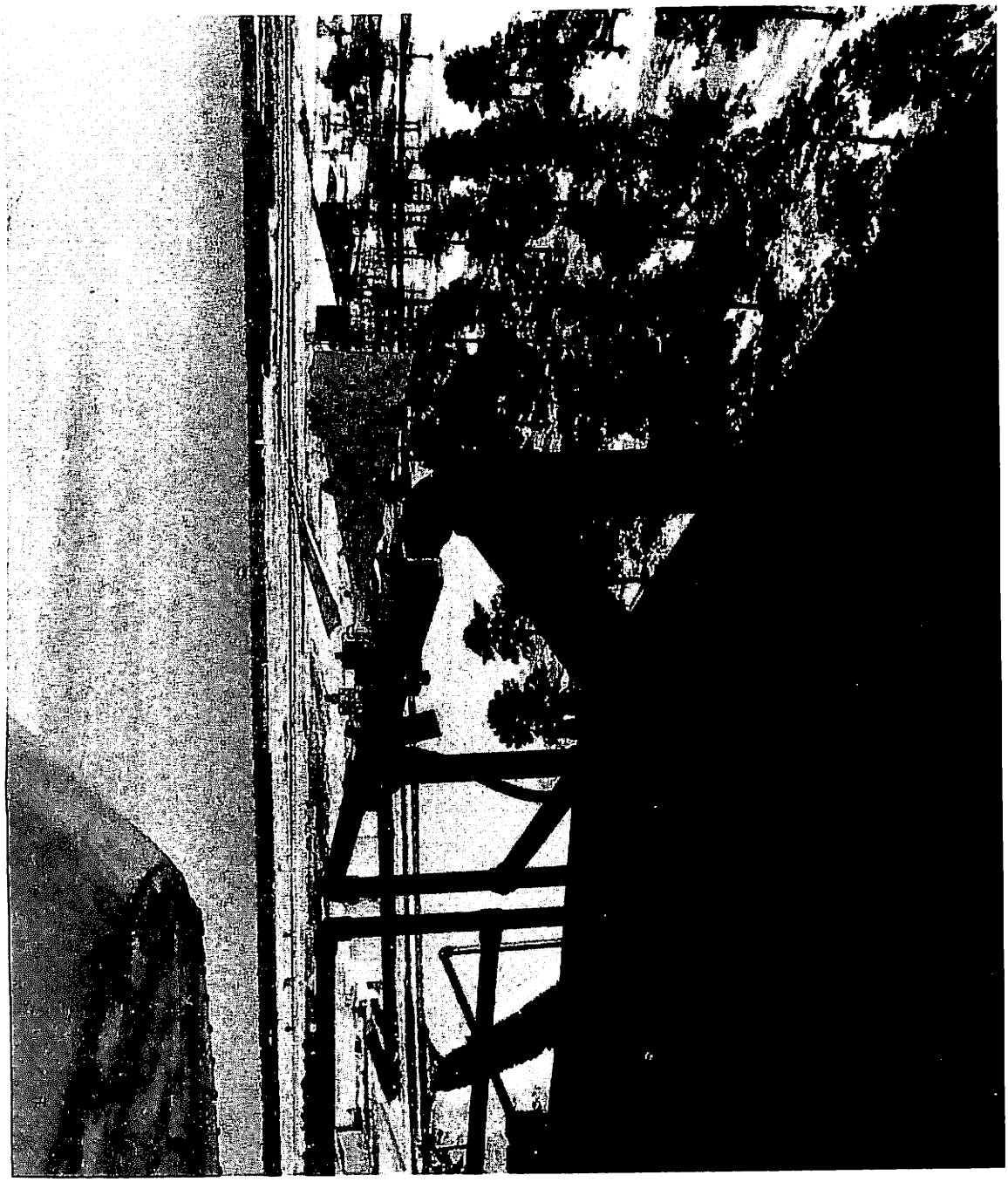

FIGURE 31. STANDARD GAIN HORN INSTALLED ON ASDE-3 TOWER

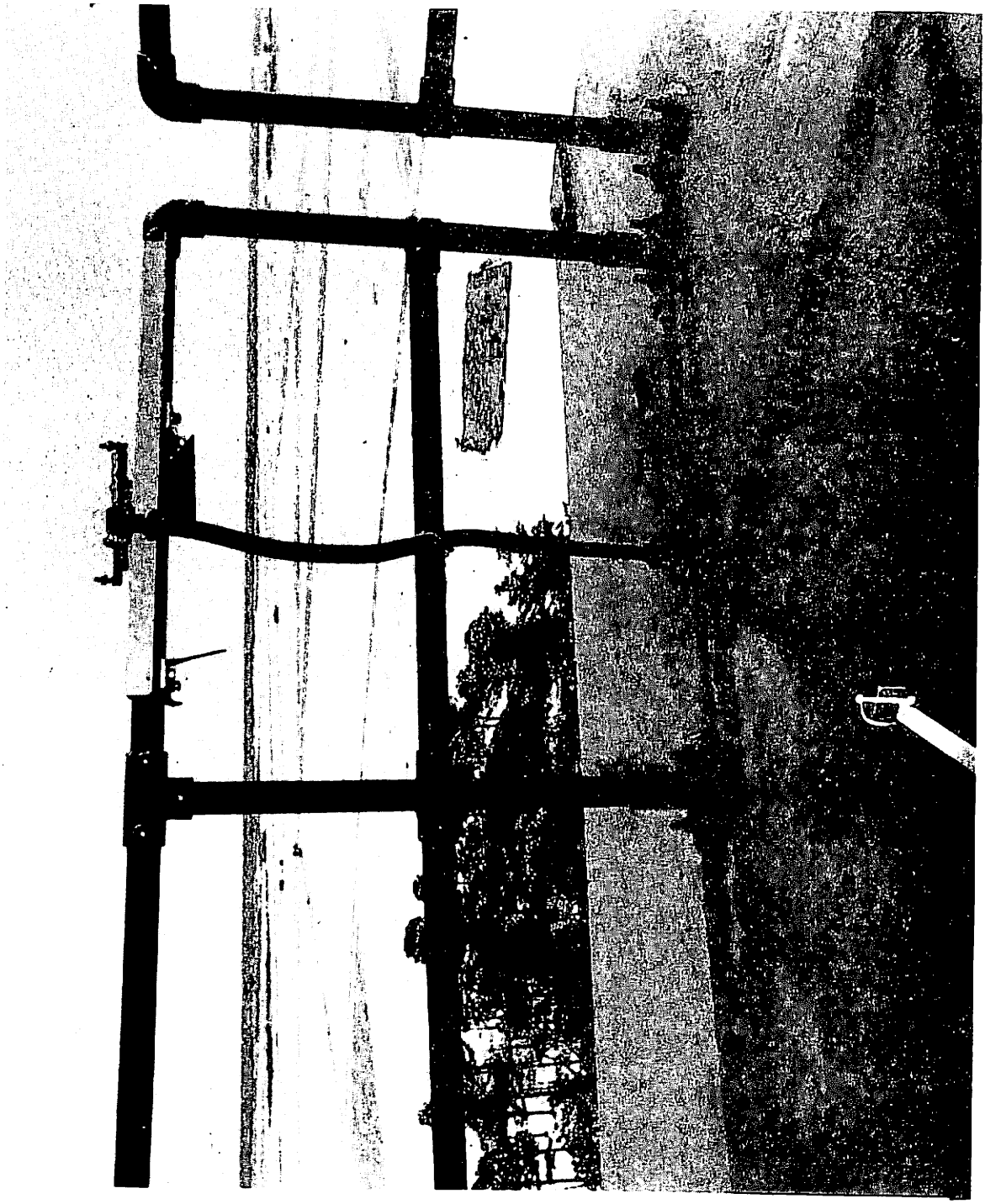

FIGURE 32. PAD #1 AND AIRPORT SURFACE AS SEEN FROM STANDARD GAIN HORN INSTALLATION

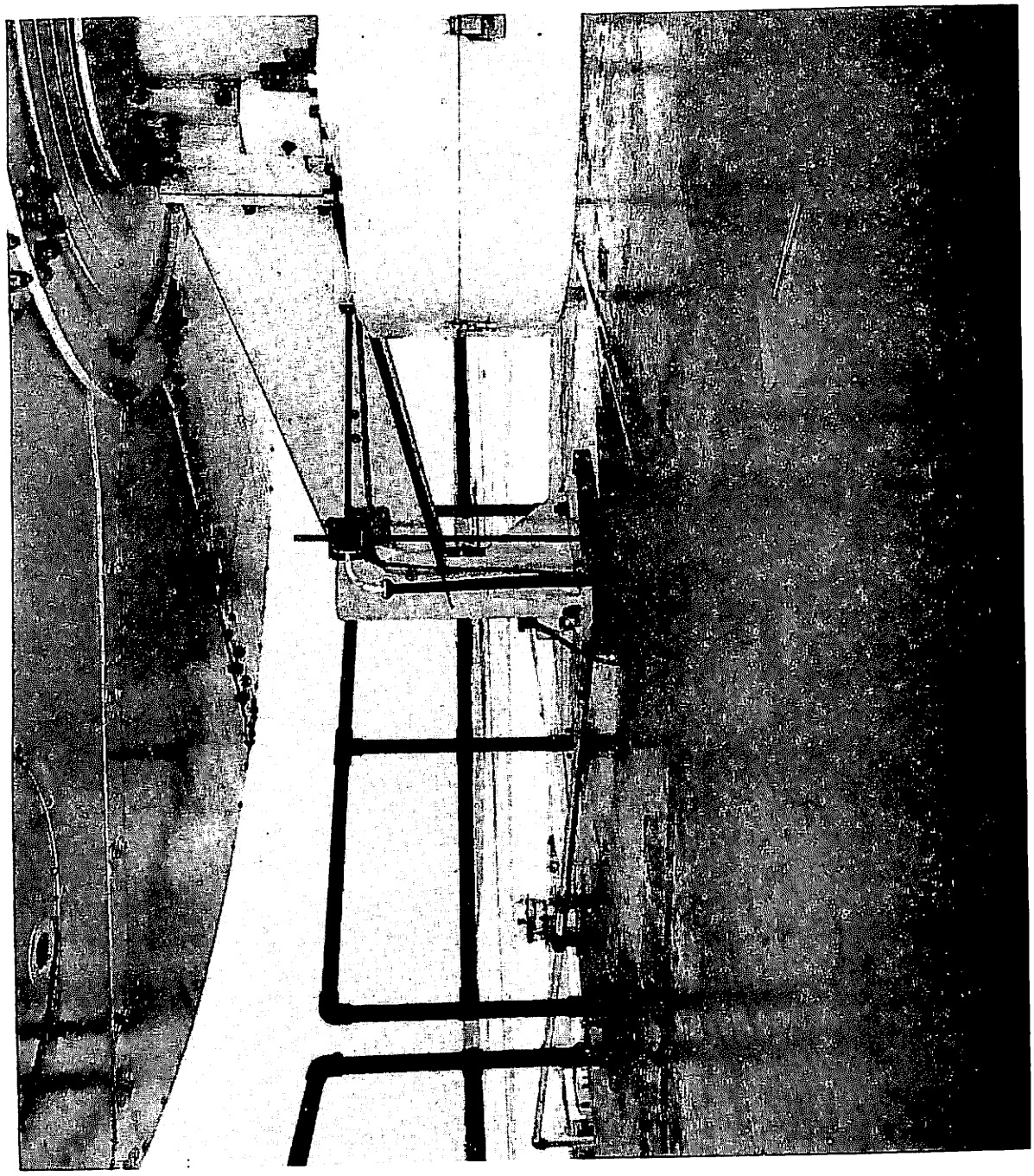

FIGURE 33. WAVEGUIDE SWITCH INSTALLED ON ASDE-3 TOWER

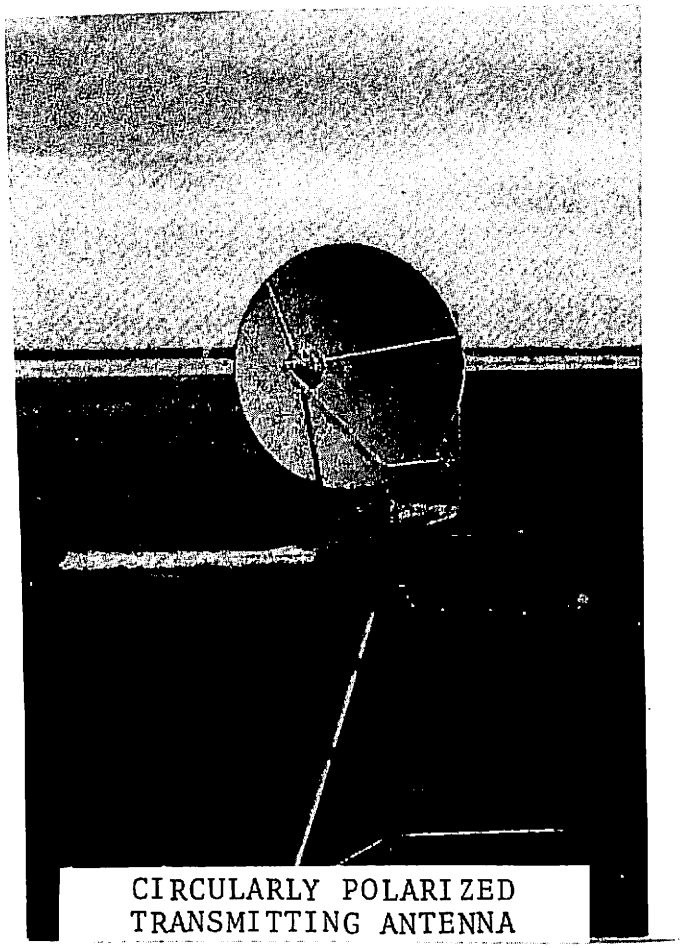

CIRCULARLY POLARIZED
TRANSMITTING ANTENNA

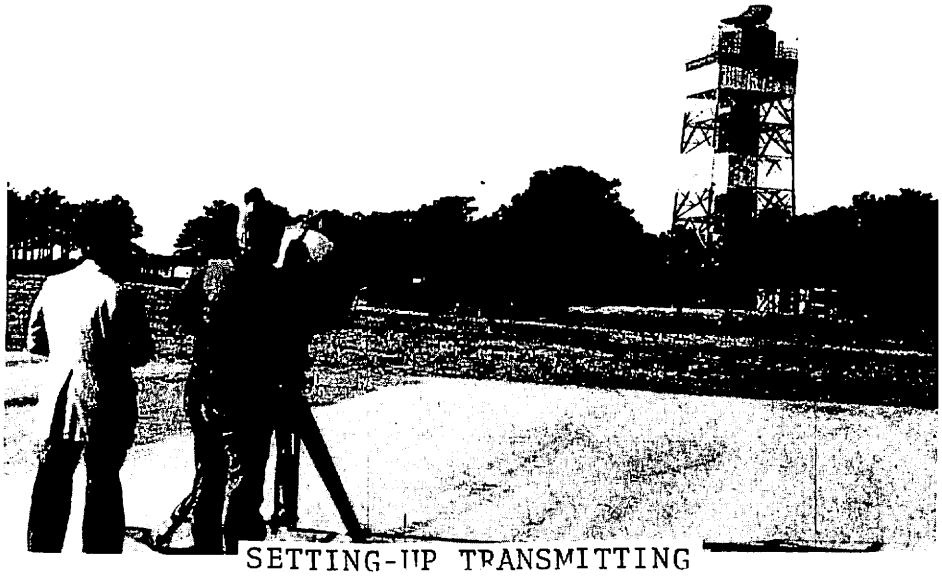

SETTING-UP TRANSMITTING
ANTENNA ON PAD #1

FIGURE 34. ASDE-3 ANTENNA PATTERN TESTING

this technique. The pattern data taken when transmitting from Pad #1 are shown in Figure 35. This pattern corresponds to a depression angle of about 11.3° and is within the near-field. The -3 dB BW measured about 0.9°. This figure is approximately 3 times the -3 dB BW measured by TM on their antenna range and tabulated in Table 2. The most disturbing fact about this pattern was the severe distortion of the azimuth beam. Radiation azimuth patterns were also taken from Pads #2 and #3. These are shown in Figures 36 and 37. The -3 dB beamwidths were 0.50° and 0.44° respectively. Slight distortion persisted in the Pad #2 pattern and to a lesser degree in the Pad #3 pattern.

It was suspected that the distortion was in some way caused by the centrifugal forces associated with the 60 rpm rotation. In order to verify this, a Cardion circuit designed for use by TM in their dynamic tests was used to allow radiation patterns to be taken at slow rotation. This circuit integrates the Azimuth Change Pulses (ACPs) from the pedestal and provides a voltage to the X-axis of the oscilloscope that is proportional to azimuth angle. Figure 38 shows the azimuth patterns from Pad #1 taken by this technique as well as the sweep technique at 62 rpm. The beamwidths measured by both techniques agree fairly well. As the antenna slowed down, the "integrated ACP technique" showed a narrowing of the beamwidth and the virtual disappearance of distortion. Figures 39 and 40 show additional patterns taken from Pads #2 and #3.

TM was contacted and asked if this variation of near-field beamwidth with rotation rate, was observed in their dynamic tests. They indicated that their dynamic tests were performed perfunctorily and with their set-up they did not notice any radiation pattern change with rotational speed.

In an attempt to fix this problem, temporary restraining brackets were installed in the rotodome to limit the deflection of the reflector tips. Patterns were retaken and the results are summarized in Table 3. The brackets narrowed the Pad #1 pattern but some distortion still remained.

VERTICAL POLARIZATION

HORIZONTAL POLARIZATION

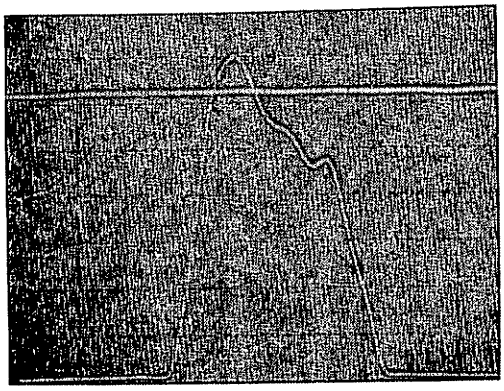

ST'D GAIN
HORN
24.7 dBi

-3 dB

-6 dB

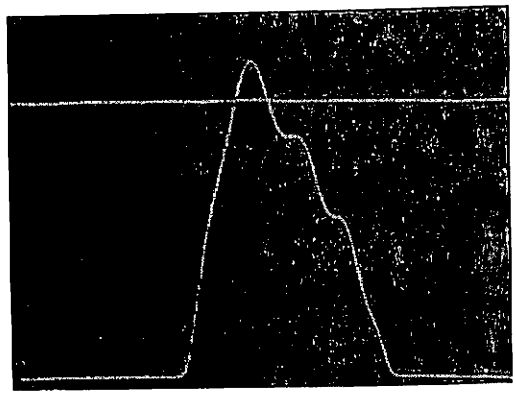

FREQ. 15.95 GHz

VERT. POL. BW = 1.0°
VERT. POL. GAIN =26 dBi
VERT. POL. SLL = -16.2dB

HORIZ. POL. BW = 0.8°
HORIZ. POL. GAIN = 26 dBi
HORIZ POL. SLL = -15.2 dB

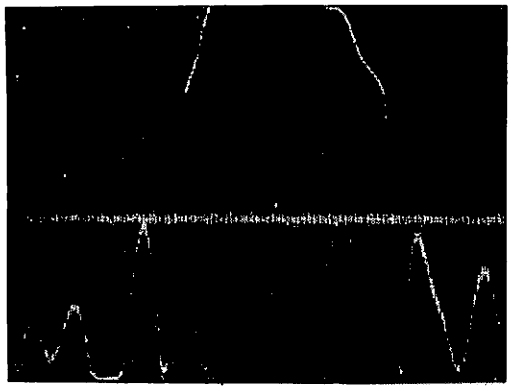

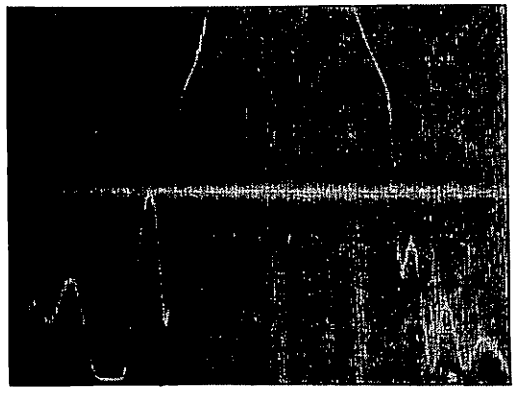

FIGURE 35. ASDE-3 ROTODOME RADIATION PATTERNS TAKEN FROM PAD #1

VERTICAL POLARIZATION

HORIZONTAL POLARIZATION

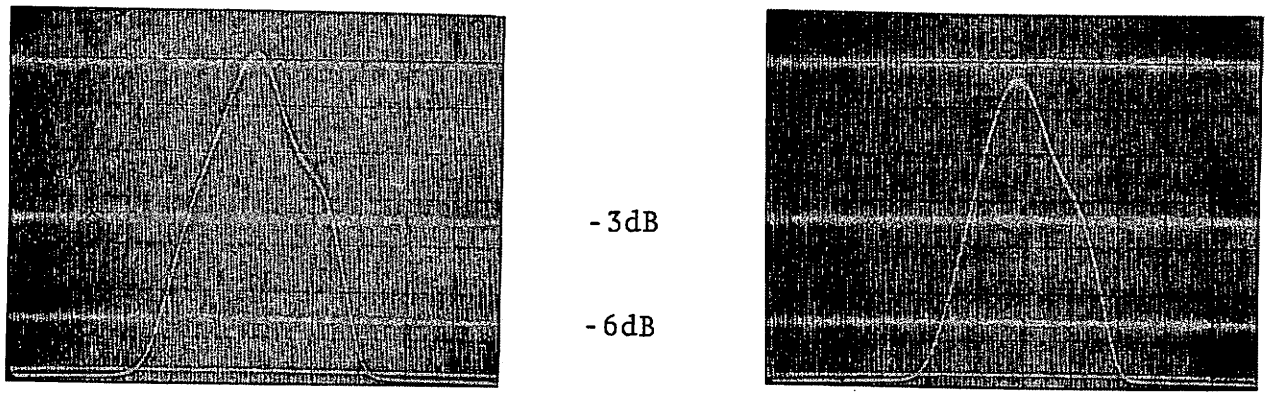

FREQ. 15.95GHz

VERT. POL. BW = 0.56°
VERT. POL. GAIN =
VERT. POL. SLL = -16.7 dB

HORIZ. POL. BW = 0.44°
HORIZ.POL. GAIN =
HORIZ. POL. SLL = -15.5 dB

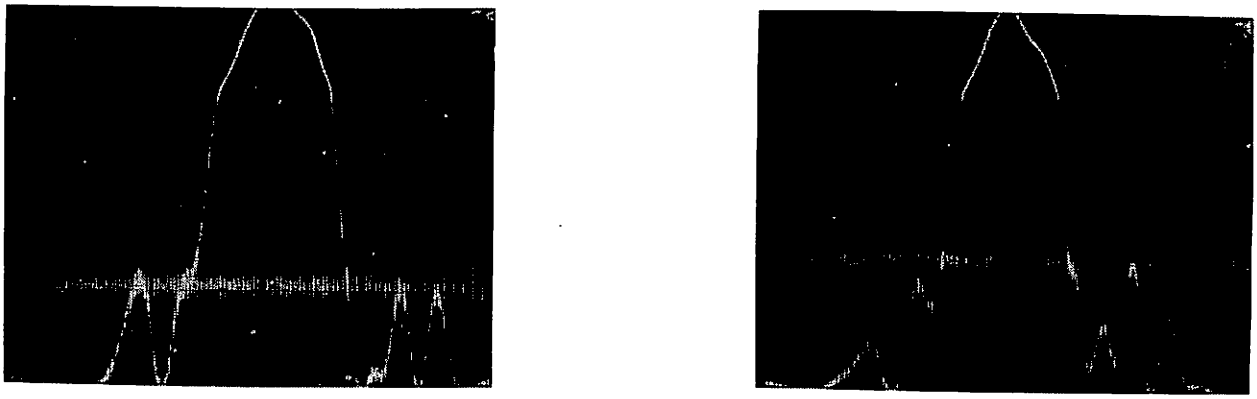

FIGURE 36. ASDE-3 ROTODOME RADIATION PATTERNS TAKEN FROM PAD #2

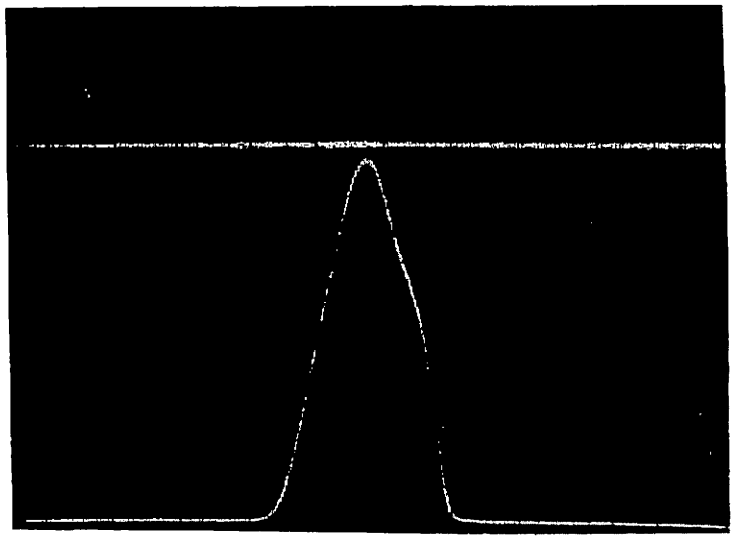

VERTICAL POLARIZATION

FREQUENCY 15.7 GHz

VERTICAL POL BW= 0.44°

FIGURE 37. ASDE-3 ROTODOME RADIATION PATTERN TAKEN FROM PAD #3

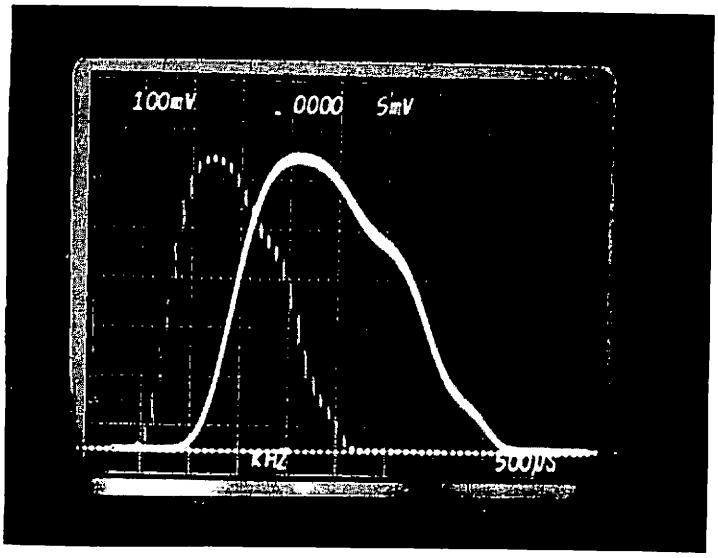

VERTICAL POL BW
62RPM
ACP TRACE BW= 0.64°
TIME TRACE BW= 0.63°

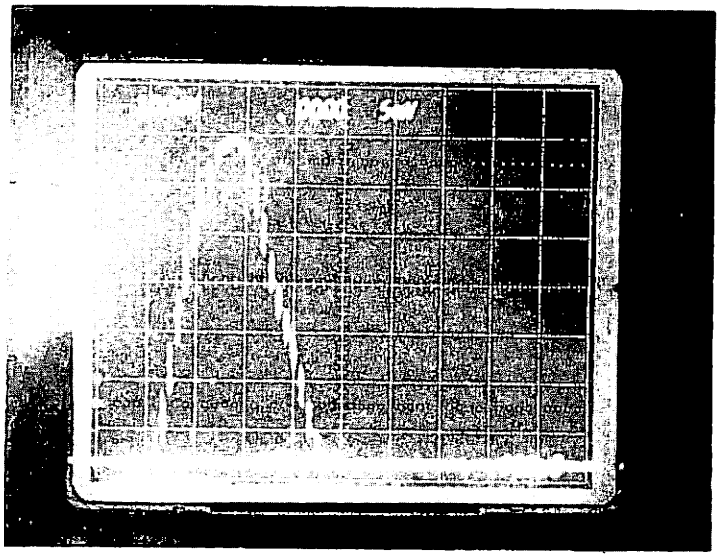

0 RPM
ACP TRACE BW= 0.40°

VERTICAL POLARIZATION

FREQUENCY 15.7 GHz

FIGURE 38. ASDE-3 ROTODOME RADIATION PATTERNS TAKEN FROM PAD #1

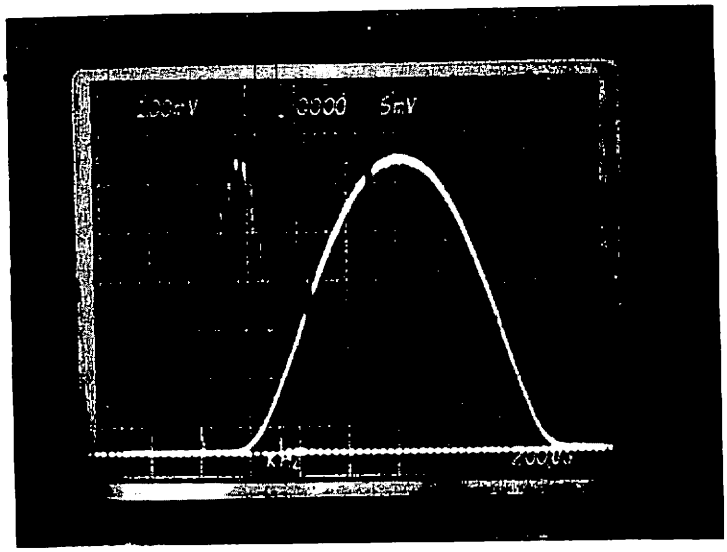

VERTICAL POL BW
62 RPM
ACP TRACE BW = 0.25°
TIME TRACE BW = 0.25°

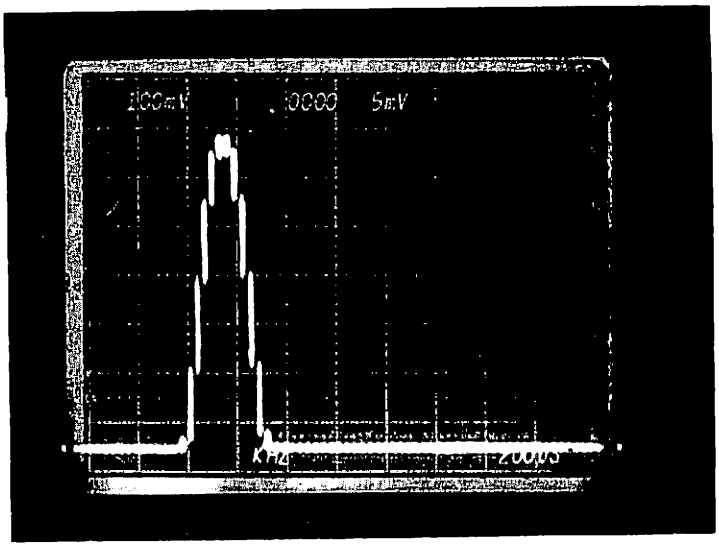

0 RPM
ACP TRACE BW = 0.25°

VERTICAL POLARIZATION
FREQUENCY 15.7GHz

FIGURE 39. ASDE-3 ROTODOME RADIATION PATTERNS TAKEN FROM PAD #2

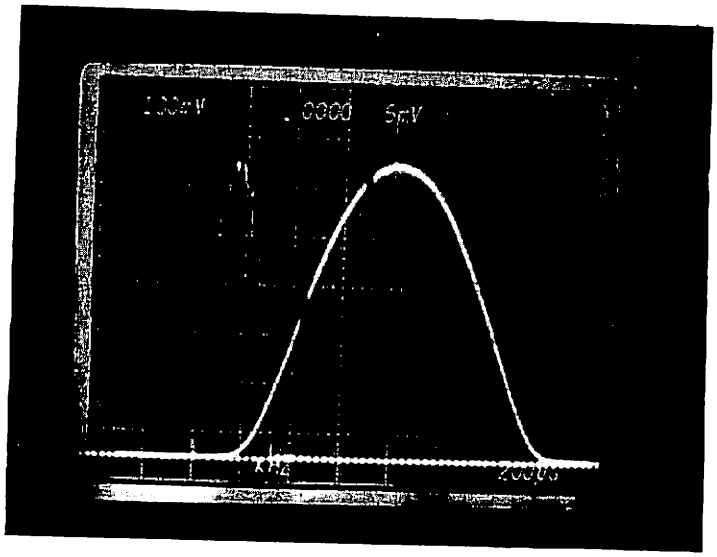

VERTICAL POL BW
62 RPM
ACP TRACE BW = 0.25°
TIME TRACE BW = 0.25°

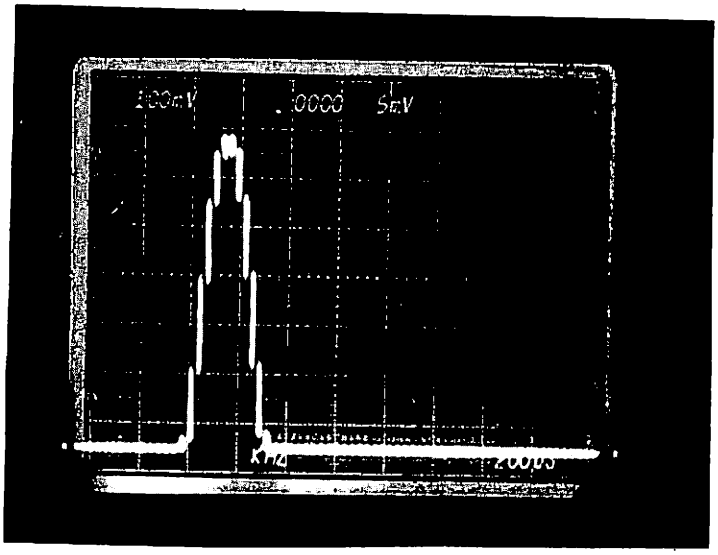

0 RPM
ACP TRACE BW = 0.25°

VERTICAL POLARIZATION
FREQUENCY 15.7GHz

FIGURE 40. ASDE-3 ROTODOME RADIATION PATTERNS TAKEN FROM PAD #3

TABLE 3. EFFECT OF ROTATION ON ROTODOME AZIMUTH BEAMWIDTH

		AZIMUTH @ 0 RPM	BEAMWIDTH @ 62 RPM
PAD #1	Reflector Not Restrained	----	0.9°
	Reflector Restrained	0.4°	0.64°
PAD #2	Reflector Not Restrained	----	0.50°
	Reflector Restrained	0.25°	0.25°
PAD #3	Reflector Not Restrained	----	0.25°
	Reflector Restrained	0.25°	0.25°

Permanent restraining brackets were subsequently installed at FAATC by T.M. They are shown in Figure 15. During this installation, various prestress conditions of the reflector were tried in an attempt to completely clear up the distortion and maintain the nominal 0.25° beamwidth throughout the near-field and far-field. When the reflector was distorted to eliminate the "defocussing" effects in the near-field, the far-field patterns became distorted. The decision was, therefore, made to accept the near-field distortion since the "spot size" although increased would still be small enough to retain the azimuth resolution at the "close-in ranges".

6.3 DAS TECHNIQUE RESULTS

When the DAS became available, attempts were made to repeat the dynamic antenna pattern tests performed with the oscilloscope technique. Considerable difficulties were encountered in performing these tests; the DAS antenna program was not optimum and required modification; heavy rains occurred during the scheduled week; and the source antenna transmitter exhibited stability problems. Consequently, a limited amount of valid data was taken, and due to schedule constraints additional test time was not available. Some data was taken from Pads #1 and #2. Typical DAS processed radiation patterns are shown in Figures 41 and 42. These radiation patterns showed the asymmetry previously observed on the dynamic patterns taken with the oscilloscope techniques. The patterns are plotted in dB's so that direct comparison with the previous dynamic pattern data is difficult. The DAS technique permits examination of the side lobe levels and provide a permanent record of the test. Repeatability of the technique can be seen in Figure 43 for both the expanded scale as well as the normal scale. The repeatability is shown in Figure 44 which shows successive radiation pattern plots taken over a period of 10 minutes and averaging the readings of 2 scans for each plot.

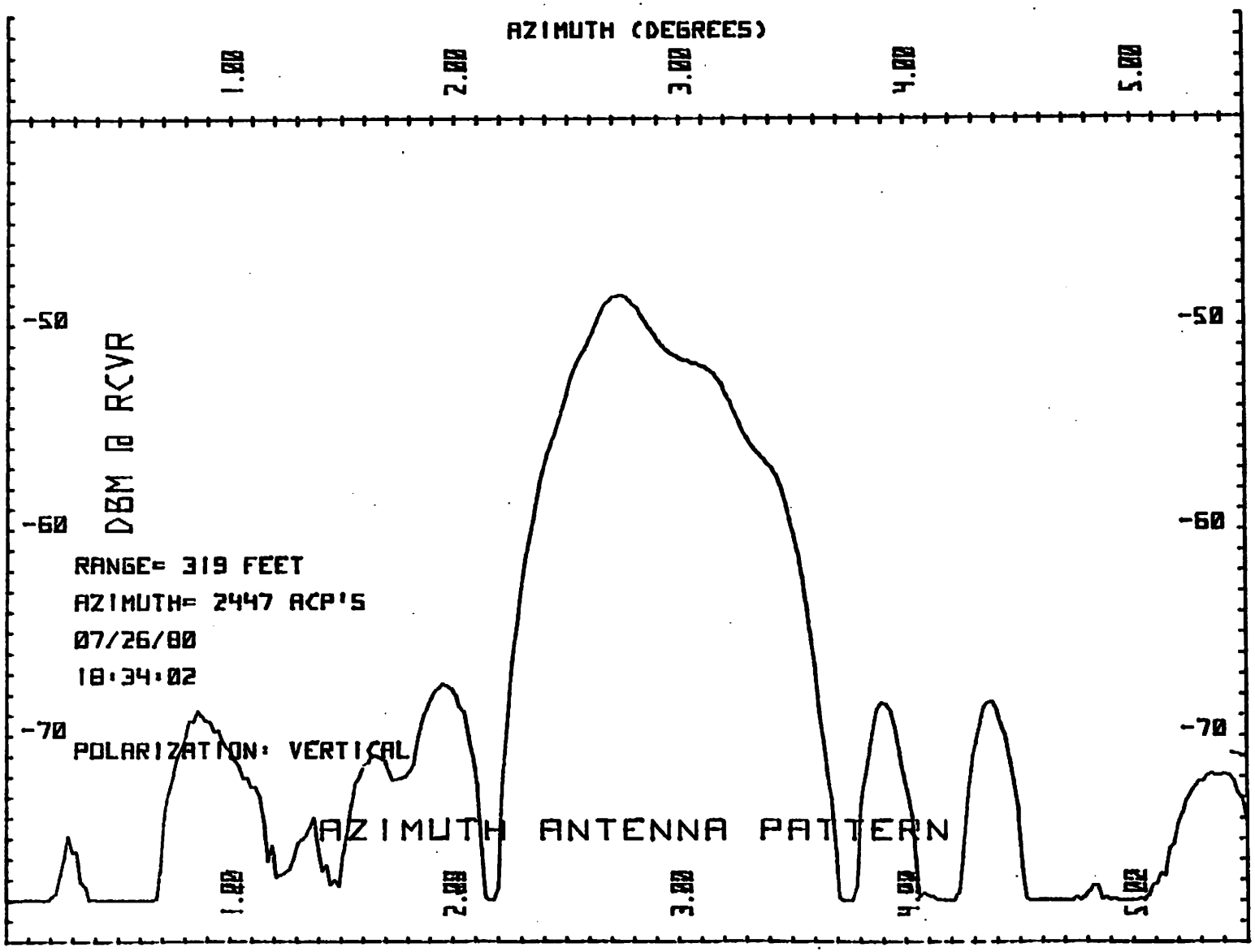

FIGURE 41. RADIATION PATTERN FROM PAD #1.

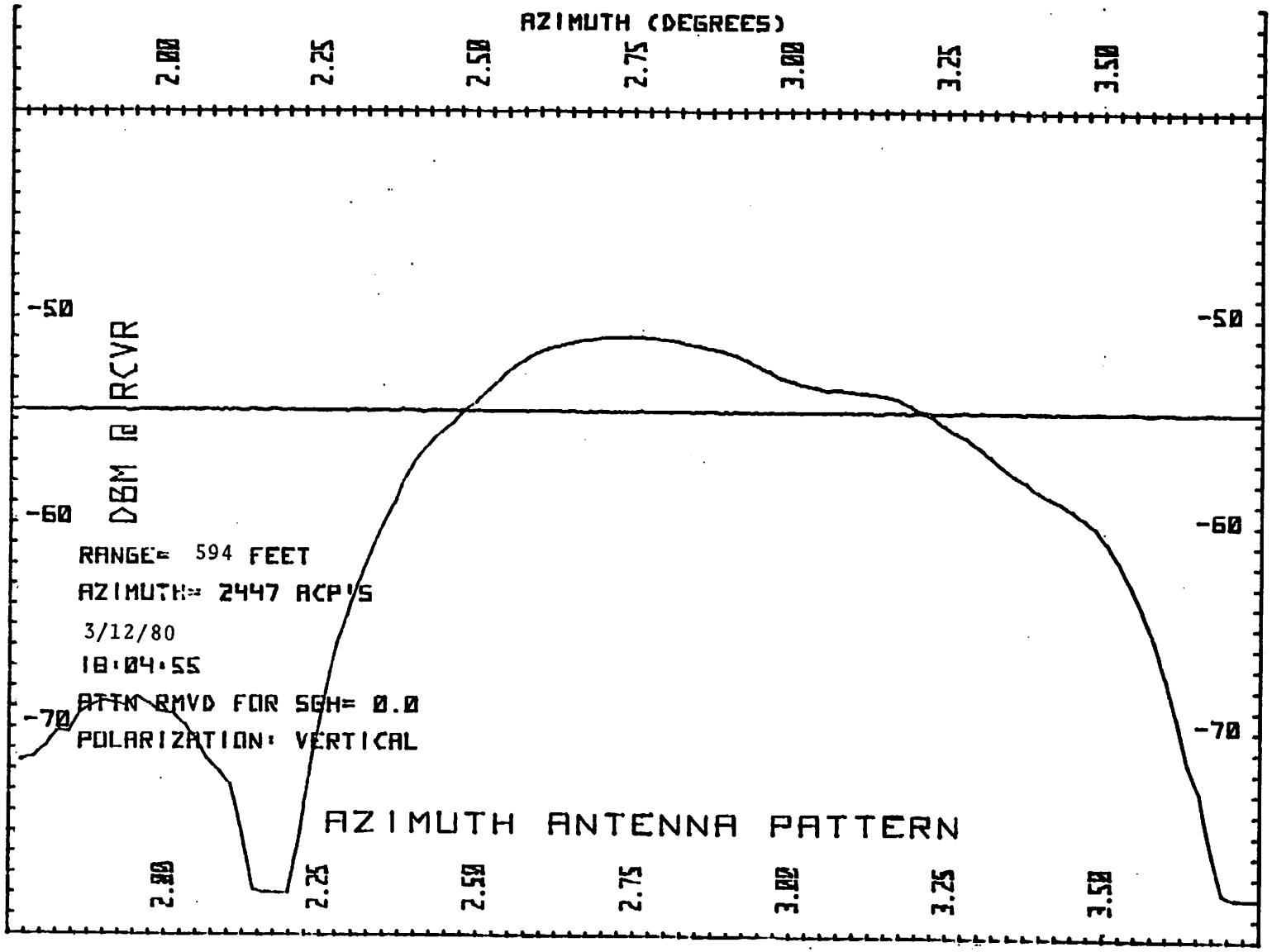

FIGURE 42. EXPANDED SCALE RADIATION PATTERN PAD #1

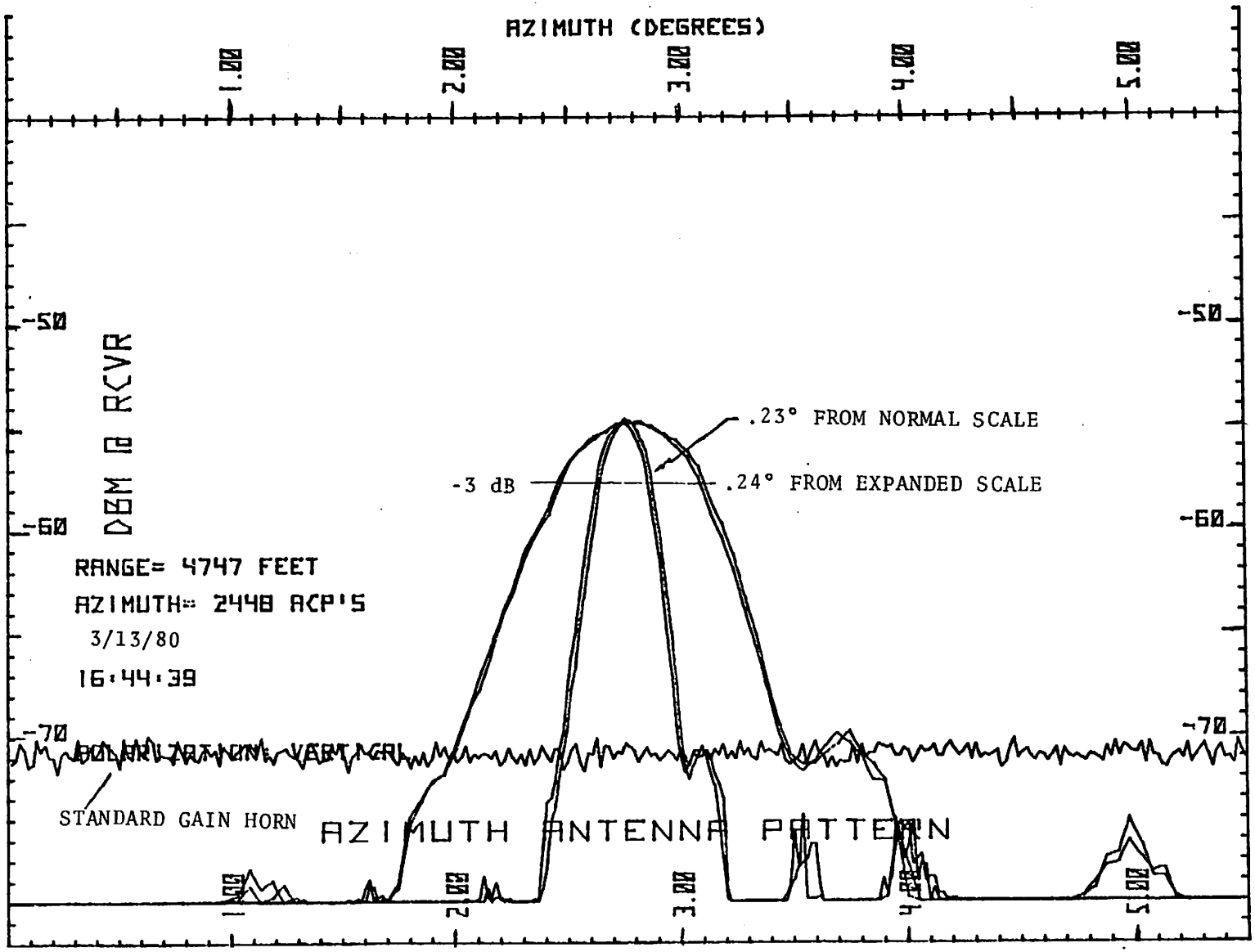

FIGURE 43. RADIATION PATTERN FROM PAD #2 (SHOWING REPEATABILITY)

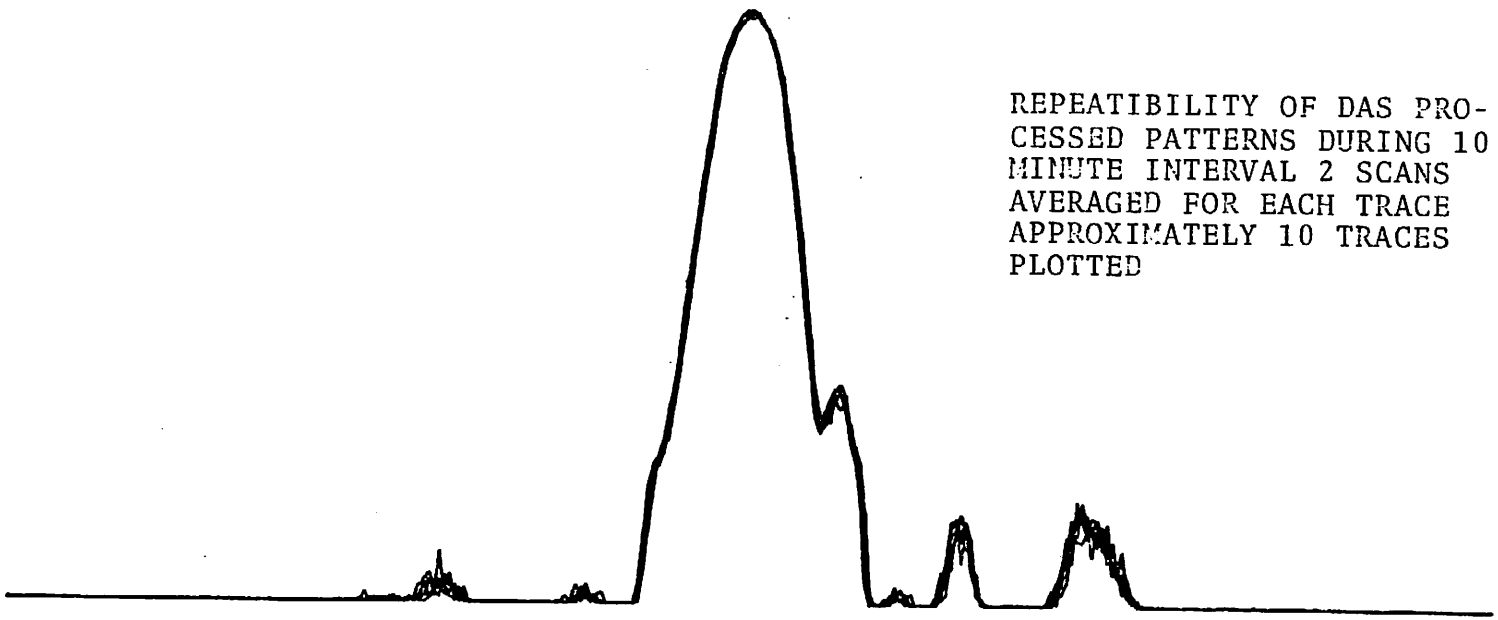

FIGURE 44. RADIATION PATTERN FROM PAD #2
(SHOWING LONGER TERM STABILITY

Although, the DAS is a very convenient and powerful technique for measuring antenna characteristics "in situ", its full potential could not be adequately exploited. Some changes on the program were required to allow operator flexibility, and although the program was later modified, a second iteration of the testing could not be performed due to schedule.

7. CONCLUSIONS AND RECOMMENDATIONS

The ASDE-3 rotodome has proved the feasibility of a new concept in high-resolution, shaped-beam antennas. It has an integral aerodynamically shaped radome that rotates with the antenna. It reduces the overturning moment of the tower equipment and because of its rotation rate, sheds the water film that forms on the outside surface of stationary radomes and which is so deleterious to radar performance at these frequencies.

The theoretical focussing properties of the reflector have been verified by computer analyses and to a limited extent by azimuth radiation pattern measurements. The gain and side lobe requirements of the specification have been met. Beamwidth and axial ratio performance was adequate but could be improved. Improvements in axial ratio are within the state of the art and should pose no serious development problem.

☆U.S. GOVERNMENT PRINTING OFFICE: 1981—701-337/42

200 copies